Linking E-cadherin mechanotransduction to cell metabolism through force-mediated activation of AMPK

Jennifer L Bays, Hannah K Campbell, Christy Heidema, Michael Sebbagh, Kris A Demali

Linking E-cadherin mechanotransduction to cell metabolism through force mediated activation of AMPK

Jennifer L. Bays[1], Hannah K. Campbell[1#], Christy Heidema[2#], Michael Sebbagh[3], and Kris A. DeMali[1,2*]

[1]Department of Biochemistry and the [2]Interdisciplinary Graduate Program in Molecular and Cellular Biology, Roy J. and Lucille A. Carver College of Medicine, University of Iowa, Iowa City, IA 52242. [3]Centre de Recherche en Cancérologie de Marseille, Aix Marseille Univ UM105, Inst Paoli Calmettes, UMR7258 CNRS, U1068 INSERM, Cell Polarity, Cell signalling and Cancer - Equipe labellisée Ligue Contre le Cancer, Marseille, France.

[#]These authors contributed equally to this work.

*Corresponding Author: Kris DeMali, Department of Biochemistry, University of Iowa, Iowa City, IA 52242, Tel:319-335-7882, Email: kris-demali@uiowa.edu

The response of cells to mechanical force is a major determinant of cell behavior and is an energetically costly event. How cells derive energy to resist mechanical force is unknown. Here, we show that application of force to E-cadherin stimulates Liver Kinase B1 (LKB1) to activate AMP-activated protein kinase (AMPK), a master regulator of energy homeostasis. LKB1 recruits AMPK to the E-cadherin mechanotransduction complex, thereby stimulating actomyosin contractility, glucose uptake, and ATP production. The increase in ATP provides energy to reinforce the adhesion complex and actin cytoskeleton so the cell can resist physiological forces. Together, these findings reveal a paradigm for how mechanotransduction and metabolism are linked and provide a framework for understanding how diseases involving contractile and metabolic disturbances arise.

In response to externally applied forces, cell surface adhesion receptors trigger robust actin cytoskeletal rearrangements and growth of the associated adhesion complex[1-3]. These changes are energetically costly, requiring approximately 50% of the total ATP in a cell[4, 5]. Energy homeostasis is controlled by AMP-activated protein kinase (AMPK). Based on this rationale, we tested whether application of force on E-cadherin

increased AMPK activity. For this, a well-established approach to directly apply force to cadherins was employed[6-12]. Magnetic beads were coated with E-cadherin extracellular domains (or IgG as a control) and permitted to adhere to MCF10A epithelial cells. A constant force was then applied for 5 minutes using a permanent ceramic magnet. Following application of force, AMPK was immunoprecipitated and subjected to an *in vitro* kinase assay with a fusion protein of GST and a SAMS peptide (an AMPK-specific substrate)[13]. Application of force increased phosphorylation of the SAMS peptide by 4.9-fold; a control peptide (SAMA) lacking the second serine phosphorylation site was not phosphorylated (Fig. 1a). Importantly, the peptide phosphorylation was blocked by application of Compound C (a cell permeable AMPK specific inhibitor)[14].

As additional measures of AMPK activation, we examined phosphorylation of AMPK in its activation loop and phosphorylation of the AMPK substrate, acetyl CoA carboxylase. Force increased phosphorylation of AMPK in its activation loop in MCF10A (pAMPK, Fig. 1b) and MDCK (Fig. S1a) cells. The increases in activation loop phosphorylation were blocked when AMPK was inhibited using shRNAs (Fig. 1b) or Compound C (Fig. S1a-c). Phosphorylation of acetyl CoA carboxylase was also elevated (Fig. S1c). Hence by three independent measures, force stimulated AMPK activation.

To ensure AMPK activation was independent of the method of force application shear stress was applied to MDCK cells using a parallel plate chamber. Alternatively, junctional assembly was triggered using a calcium switch assay—a process that relies on elevations in actin polymerization and myosin II activity[15, 16]. Both shear stress and junctional assembly stimulated AMPK activation loop phosphorylation (Fig. 1c,S1d).

To interrogate the contribution of E-cadherin to force-induced AMPK activation, we examined the effects of inhibiting E-cadherin function using a function blocking antibody (HECD-1) or by silencing E-cadherin expression (Fig. 1d, S1e). E-cadherin was required to trigger AMPK activation (Fig. 1d, S1e). Additionally, application of force to another transmembrane adhesion receptor, syndecan-1, failed to enhance AMPK

phosphorylation (Fig. S1f). Taken together, these data demonstrate that force on E-cadherin stimulates AMPK activation.

To investigate the contribution of force to AMPK activation, we examined the effect of promoting and interfering with known mechanically controlled elements. To promote force transmission increases in contractility were stimulated by applying Calyculin A, a phosphatase inhibitor that augments myosin II phosphorylation. Stimulating myosin light chain phosphorylation increased AMPK activation (Fig. 1e). To interfere with force transmission, cells were treated with blebbistatin, a myosin II inhibitor. In the presence of blebbistatin, myosin light chain phosphorylation and force-induced AMPK activation were decreased (Fig. 1d).

Since activate AMPK localizes to the plasma membrane[17] and E-cadherin is membrane-bound[18, 19], we examined whether force stimulated AMPK recruitment to the cadherin adhesion complex. To address this possibility, we applied tensile forces to E-cadherin and the level of co-precipitating AMPK and activated AMPK were assessed. AMPK (Fig 1f) and active AMPK (Fig 1g) were recovered with E-cadherin complexes. The recruitment of AMPK to E-cadherin was blocked by preincubation of the cells with blebbistatin (Fig 1f and g), with E-cadherin function blocking antibodies (Fig 1f and g), or by silencing AMPK expression (Fig S1g). Additionally, the recruitment of AMPK to E-cadherin was not dependent on the method of force application as stimulating junctional assembly using a calcium switch assay triggered AMPK co-immunoprecipitation with E-cadherin (Fig. S1h). Taken together, these studies demonstrate AMPK is recruited to E-cadherin in response to force.

How is AMPK activated and recruited to the cadherin complex? Previous studies from the Schwartz laboratory indicated that LKB1, an AMPK activator, localizes to cadherin-containing complexes in maturing junctions[17]. Additionally work from Cantley laboratory found that calcium-induced tight junction assembly depends on LKB1[20]. Based on this rationale, we determined if LKB1 associates with the cadherin adhesion complex in response to force. LKB1 was recovered with E-cadherin-coated magnetic

beads in a force- and E-cadherin-dependent manner (Fig 2a). Since the buffer conditions used to examine protein recruitment beneath the magnetic beads were less strigent than convention co-immunoprecipitation studies, we examined if LKB1 co-immunoprecipitated with E-cadherin. Robust co-immunoprecipitation of E-cadherin was observed LKB1 immunoprecipitates recovered from cells lysed in a 1%-triton x100-containing buffer, thereby confirming the interaction (Fig 2b). In further support of LKB1, we determined if LKB1 co-localized with E-cadherin in cells. Since the magnetic beads we use in these studies autofluorescence, we examined co-localization in response to application of shear stress to MDCK cells. We observed strong co-localization of LKB1 and E-cadherin (Fig 2c).

Having identified a mechanically-active signaling pathway from E-cadherin to LKB1, we next determined if LKB1 is required for AMPK activation and recruitment to the cadherin adhesion complex. Tensile forces were applied to E-cadherin on MCF10A (Fig 2d) or on MDCKII (Fig 2e) cells. We found the force-induced activation of AMPK was prevented by LKB1 silencing in both cell lines (Fig 2d-e). Similarly, shear stress-induced activation of AMPK was blocked by inhibition of LKB1 (Fig 2f). We next determined whether LKB1 was required for the recruitment of AMPK to E-cadherin. LKB1 inhibition prevented co-precipitation of AMPK and active AMPK with E-cadherin coated magnetic beads (Fig 2g). Taken together, this data demonstrates that LKB1 is needed for AMPK to be recruited to and activated at cadherin-containing sites.

The observation that LKB1 and AMPK are recruited to the cadherin adhesion complex suggests they may lie in a known contractility pathway. This pathway initiates when E-cadherin activates Abelson tyrosine kinase (Abl) thereby triggering phosphorylation of Y822 vinculin (Fig. 3a) and culminating in elevated RhoA-mediated contractility[11]. To determine whether LKB1 and/or AMPK are components of this pathway, we examined the effect of their inhibition. As an indicator of Abl activation, we followed phosphorylation the Abl substrate, CrkL, using a phosphospecific antibody against the Abl-specific sites[21]. Application of tensile forces using the magnetic bead approach stimulated CrkL phosphorylation in MCF10A (Fig 3b and c) and MDCKII cells

(Fig. S2a). Inhibition of LKB1 (Fig. 3b, S2a) or AMPK (Fig. 3c, S2b) prevented this increase. Stimulation of vinculin Y822 phosphorylation, a downstream target of Abl, also required LKB1 (Fig. 3d) and AMPK (Fig 3e, S2c). These data indicate that AMPK lies upstream of Abl in the known contractility pathway. Since Abl is activated and AMPK and vinculin are recruited to cadherin-containing junctions in response to force[22], we examined whether AMPK is in a complex with these components. For this, we monitored co-immunoprecipitation of vinculin and Abl with AMPK from cells lysed in RIPA buffer. These studies revealed that AMPK forms a complex with Abl and vinculin in a force-dependent manner (Fig. 3f).

Further downstream in the E-cadherin contractility pathway (Fig. 3a), RhoA-mediates activation of Rho kinase, which promotes phosphorylation of myosin light chain (MLC), thereby stimulating actomyosin contractility[23]. We measured force-induced RhoA activity in cells in the presence or absence of LKB1 or AMPK. Application of tensile force to E-cadherin stimulated RhoA activation in an LKB1- and AMPK-dependent manner (Fig. 3g). To determine if increases in RhoA were propagated to changes in contractility, we analyzed MLC phosphorylation at a regulatory Ser19 site[24]. MLC phosphorylation increased 2.7-fold in response to force (Fig 3h). Inhibition of AMPK or LKB1 abrogated these effects (Fig. 3g, 3h, S2d, and S2e). Taken together, these findings demonstrate that AMPK is required to increase RhoA-mediated contractility when E-cadherin experiences force.

These observations raise the question why cells activate a master regulator of metabolism, such as AMPK, to modulate contractility. When cells experience force, elevations in enzymatic activity, actin polymerization, and actomyosin contractility facilitate the cytoskeletal rearrangements and the growth of adhesions necessary to withstand the force[2, 25-28]. All of these processes require energy. The preferred energy source for epithelial cells is ATP derived from glucose oxidation[29]. In other systems, AMPK activation stimulates glucose uptake and oxidation[30]. Based on this rationale, we hypothesized a consequence of force-induced AMPK is the stimulation of glucose uptake. To test this possibility, tensile forces were applied to E-cadherin and the uptake

of a fluorescently labelled, non-hydrolyzable 2-deoxyglucose was monitored. Force stimulated a 2.2-fold increase in glucose uptake in the MCF10A cells (Fig. 4a, Fig. S3a) and a 2.6-fold increase in the MDCK II cells (Fig. 4b, Fig. S3b). Moreover, inhibition of E-cadherin, LKB1, or AMPK prevented the force-induced glucose uptake (Fig. 4a-b, Fig. S3a-b). To ensure that these results were not the consequence of the approach, the effects of shear stress on MDCKII cells or the effects of stimulating junctional assembly (using a calcium switch assay) were monitored. Both methods stimulated an elevation in glucose uptake. The fold activation was similar to the increase observed when tensile forces applied (Fig. 4c, S3c, S3d) and required E-cadherin, LKB1 and AMPK. Collectively, these data demonstrate that force on E-cadherin stimulates glucose uptake in a LKB1- and AMPK-dependent manner.

In response to many stimuli, glucose is oxidized to ATP. Hence, we tested whether increases in glucose uptake translate to elevations in ATP. Application of force to E-cadherin increased cellular ATP levels by 1.5-fold (Fig. 4d and S3e). The increase in ATP, while slight, was statistically significant and reproducible (Fig. S3e). This modest change is not surprising as ATP levels remain relatively constant, even in the most metabolically active tissues[31]. Importantly, we found force-induced ATP could be blocked by the shRNAs against LKB1 or AMPK (Fig 4d), the AMPK inhibitor Compound C (Fig. 4e, Fig S3f), or the ATP synthase inhibitor Oligomycin A (Fig. 4e, Fig S3f). To ensure that the ATP produced was derived from glucose, the effect of a non-hydrolyzable, 2-deoxyglucose analog was studied. The 2-deoxyglucose analog blocked force-induced elevations in ATP (Fig. 4e). Taken together, these data indicate that the glucose taken up when E-cadherin experiences force is converted to ATP.

We next tested the possibility that ATP provides the energy necessary to reinforce the actin cytoskeleton and cadherin adhesion complex in response to force. In support of a role for AMPK, we found that A-769662, an AMPK activator, increased E-cadherin and F-actin enrichment in cell-cell junctions (Fig. S4a). To directly test the role for LKB1 and AMPK, we applied shear stress to MCDK cells and monitored F-actin and E-cadherin enrichment in cell-cell junctions using immunofluorescence. A 2.0-fold

increase E-cadherin deposition in cell-cell junctions (Fig. 5a and b) and a 3.8-fold increase in junctional actin were observed in cells exposed to shear (Fig 5a and c). These increases were blocked by shRNAs against LKB1 or inhibitors of AMPK (Fig 5a-c). Similarly, inhibiting glucose metabolism (by incubating cells in low glucose containing media) or blocking ATP synthesis (using Oligomycin A or Carbonyl cyanide-4-(trifluoromethoxy)phenylhydrazone) dramatically impaired junctional enrichment of F-actin and E-cadherin in shear stress treated cells (Fig. 5a-c). Only modest changes were observed in control cells (Fig. S4b-d).

To ensure that shear stress applied force to cell-cell junctions, we investigated whether myosin light chain was phosphorylated in response to shear and whether vinculin (an actin binding protein that bears force) was enriched in cell-cell junctions. Both myosin light chain phosphorylation and vinculin localization to cell-cell contacts were increased in response to shear stress (Fig. S4e-h). In further support of a role for force, we found that the enrichment of vinculin in cell-cell junctions was blocked by preincubation of cells with blebbistatin (Fig. S4e-g). This observation is in agreement with previous findings showing vinculin is recruited to endothelial cell-cell junctions in a tension-dependent manner[32] and force-dependent vinculin recruitment can be blocked by blebbistatin[22]. Collectively, these data demonstrate that AMPK-dependent increases in ATP enrich F-actin and E-cadherin in response to force.

Previous studies show that tension is required for the formation of an epithelial barrier[33]. To interrogate the physiological significance of the pathway uncovered in this study, the formation of an epithelial barrier was monitored in MDCKII cells after a calcium switch. After readdition of calcium to the medium, control cells gradually formed an epithelial barrier (Fig. 5d). Inhibition of E-cadherin, LKB1, or AMPK or Blebbistatin compromised formation of the barrier function. By 24 h after junctional assembly was initiated, the cells with E-cadherin, LKB1 or AMPK inhibited had only modest (but statistically significant) alterations in their barriers (Fig. 5d). Interestingly, a slight alteration in barrier function at 24h after calcium readdition was observed in the MCDKII cells lacking E-cadherin. The requirement for AMPK is in good agreement with previous

studies showing that treatment of epithelial cells with AMPK activators promoted barrier function[34]. Taken together, these data indicate force-induced activation of LKB1/AMPK is required for efficient formation of an epithelial barrier.

Cell differentiation, proliferation, gene expression and disease development are all impacted by the forces experienced by the cell[35-38]. A vast literature shows that cells withstand forces by reinforcing their actin cytoskeletons and growing their adhesion complexes[1-3, 26]. These events increase enzymatic activity, actin polymerization, and actomyosin contractility[26-28], yet it is unknown how the cell derives the vast amount of energy it needs to support these events. Here, we demonstrate that LKB1-mediated activation of AMPK is a key player in a junctional contractility pathway that increases glucose uptake and ATP synthesis. This is a mechanism for how cells signal to increase energy and use the energy to reinforce their cytoskeletal networks in order to resist applied forces.

This work establishes AMPK as a critical link between mechanotransduction and metabolism. This information may serve as the impetus for future studies aimed at establishing further links between mechanotransduction and the metabolic machinery and defining mechanisms of regulation. This work also has the potential to have far reaching medical implications as AMPK is a negative regulator of diseased states with metabolic disturbances. Our observation that E-cadherin force transmission activates AMPK demonstrates that mechanical forces on E-cadherin may protect against the metabolic disturbances associated with diseases such as cardiovascular disease[39], diabetes[40], and cancer[38].

Affiliations: Department of Biochemistry, Roy J. and Lucille A. Carver College of Medicine, University of Iowa, Iowa City, IA, 52242.

Contributions: J.B. designed and performed experiments, analyzed all the data, and helped write the manuscript. C.H. and H.C. helped with experimental design and procedures. K.D. helped with the experimental design, wrote the manuscript, and directed the project. All authors provided detailed comments.

Acknowledgements: We thank Thomas Moninger and Todd Washington at the University of Iowa for their assistance in performing experiments. Research reported in this publication was supported by The National Institutes of General Medicine (Award Number R01GM112805 to K.A.D) and the National Cancer Institute of the National Institutes of Health (Award Number P30CA086862). Predoctoral fellowships from the American Heart Association (Award Number AHA 16PRE26701111) and National Institutes of Health (Award T32 GM067795) support J.B. and C.H., respectively. M.S. supported by "Fondation ARC pour la Recherche sur le Cancer" (ARC SFI20111203781) and CNRS-AMI Mecanobio (Mecanopol_2016-2017).

Figure Legends.

Figure 1. AMPK is activated in response to force applied to E-cadherin. a and b, MCF10A cells were incubated with magnetic beads coated with IgG or E-cadherin extracellular domains (E-cad). The cells were left resting(-) or a magnet was used to generate tensional forces (+). **a**, AMPK immunoprecipitates were subjected to in vitro kinase assay with its substrate, SAMS peptide. SAMA=control peptide. Cmpd. C indicates cells pretreated with the AMPK inhibitor, Compound C. **b**, total cell lysates were immunoblotted with antibodies that recognize AMPK or AMPK phosphorylated in its activation loop (pAMPK). shControl indicates cells treated with scrambled shRNAs. shAMPK1and shAMPK2 indicate cells infected with two separate shRNAs targeting AMPK. **c**, shear stress was applied to MDCK cells, and AMPK and pAMPK were monitored by immunoblotting. **d,** tensional forces (+) were applied to MCF10A cells pretreated with blebbistatin (Blebbi) or E-cadherin function blocking antibodies (HECD-1). Total cell lysates were probed with antibodies against pAMPK, AMPK, phospho-myosin light chain (pMLC), or MLC. **e,** MCF10A cells were left resting (-) or treated (+) with Calyculin A (to stimulate myosin II-dependent increased contractility). Total cell lysates were immunoblotted as described in d. **f and g,** Tensional forces were applied to MCF10A cells as described in a. The beads were recovered and co-precipitation of AMPK (f) and pAMPK (g) with E-cadherin were examined by immunoblotting. The graphs beneath the image show the average ± SEM for 3 independent experiments. *, #, and ## indicate p-values of <0.01, 0.05 and 0.005, respectively. Unprocessed scans of blots are shown in Supplementary Figure 5.

Figure 2. LKB1 is recruited to the cadherin adhesion complex in response to force and activates and recruits AMPK. MCF10A cells (a,b,d,g) or MDCK cells (e) were incubated with beads coated with IgG or E-cadherin extracellular domains (E-cad) and left resting (-) or stimulated (+) with tensional force using a permanent magnet. In other experiments, MDCK cells (c and f) were left resting (-) or exposed to shear stress (+). **a**, the cells were lysed and co-precipitation of LKB1 with the E-cadherin-coated magnetic beads was examined. **b**, Co-immunoprecipitation of E-cadherin (E-cad) with LKB1 was monitored using immunoblotting. **c**, The cells were fixed, permeabilized and stained with antibodies against E-cadherin or LKB1. The co-localization of LKB1 with E-cadherin was examined using confocal microscopy. Scale

bar = 20μm. **d-f**, The cells were lysed, and whole cell lysates were immunoblotted with the indicated antibodies. shLKB1 denotes cells with LKB1 silenced. shLuc indicates cells expressing a vector control cDNA, and cl.11 and cl.14 indicate two clonal cell lines lacking LKB1. **g**, the cells were lysed, and pAMPK and AMPK co-purification with the E-cadherin-coated magnetic beads was examined by immunoblotting. The graphs beneath each image show the average ± SEM for 3 independent experiments.* and # indicate p-values of <0.01, and <0.05, respectively. Unprocessed scans of blots are shown in Supplementary Figure 5.

Figure 3. LKB1 and AMPK are upstream of Abl-mediated phosphorylation of Y822 vinculin and Rho-mediated contractility. a, schematic of the signal transduction cascade from E-cadherin to Rho-mediated contractility. **b-h**, MCF10a cells were incubated with beads coated with IgG or E-cadherin extracellular domains (E-cad) and left resting (-) or stimulated (+) with tensional force using a permanent magnet. **b,c,d,e**, whole cell lysates were probed by immunoblotting with antibodies that recognize phosphorylation of CrkL at the Abl-specific site (b and c, pCrkL) or phosphorylation of vinculin Y822 (d and e, pY822). **f**, AMPK was immunoprecipitated and vinculin and Abl recruitment were examined by immunoblotting. **g**, Active Rho (Rho–GTP) was isolated with GST–RBD and analyzed by western blotting. **h**, total cell lysates were immunoblotted with antibodies against myosin light chain (MLC) or MLC phosphorylated at Serine 19 (pMLC). shLKB1 denotes cells expressing shRNAs against LKB1. shControl indicates cells treated with scrambled shRNAs. shAMPK1and shAMPK2 indicate cells infected with two separate shRNAs targeting AMPK. The graphs beneath each image show the average ± SEM for 3 independent experiments. **, * and # indicate p-values of <0.001, <0.01, and 0.05, respectively. Unprocessed scans of blots are shown in Supplementary Figure 5.

Figure 4. Force-induced AMPK stimulates glucose uptake and increases intracellular ATP levels. a and b, MCF10A (**a**) or MDCK (**b**) cells were incubated paramagnetic beads coated with IgG or E-cadherin extracellular domains (E-cad). Tensile forces were applied to the beads using a magnet, the cells were lysed, and the amount of a fluorescently-labelled 2-deoxyglucose analog taken up into the cells was monitored using a fluorimeter. **c**, MDCK cells were left resting (no shear) or exposed to shear stress (shear), and the amount of glucose taken up into the cells was monitored as described in a. **d** and **e,** Total ATP levels in cells treated as described in a and b were monitored as described in the experimental procedures. Cmpd C indicates cells treated with the AMPK inhibitor Compound C, Oligo indicates cells treated with the ATP synthase inhibitor, Oligomycin A, and 2-DG indicates cells incubated in the presence of 2-deoxyglucose. The graphs represent average glucose uptake or intracellular ATP for at least three representative experiments ± SEM. # and ## indicate p-values of <0.05 and < 0.005, respectively. n.s. indicates that there is no statistical differences between groups.

Figure 5. Force-induced increases in ATP reinforce the actin cytoskeleton and the E-cadherin adhesion complex to modulate barrier formation. a-c, MDCKII cells (n=80) or two

clonal MDCKII cells lines (cl.11 and cl.14, n=63 and 52 respectively) lacking LKB1 were left untreated, treated with inhibitors of AMPK (Compound C=Cmpd. C, n=62) or ATP synthesis (Oligo A,n=44 or Carbonyl cyanide-4-(trifluoromethoxy)phenylhydrazone=FCCP, n=26, or incubated in low glucose containing media (Low Gluc, n=25). The cells were then left resting (no shear) or exposed to physiological shear stress. The cells were fixed, stained with antibodies against E-cadherin or Texas-Red phalloidin, and examined by confocal microscopy. The graphs in b and c represent the average corrected fluorescence intensity of E-cadherin (b, E-cad) or F-actin (c) in junctions.The data are represented as a box and whisker plot with median, 10^{th}, 25^{th}, 75^{th}, and 90^{th} percentiles shown. Scale bars=20 μm. **d**, MDCKII cells were grown to confluence and then incubated overnight in low calcium containing media. The formation of cell-cell junctions was then stimulated by adding growth media to the cells. The trans-epithelial resistance across the epithelial monolayer was monitored using a voltmeter at the indicated times (hours). **,*, and # indicate p-values of <0.001, <0.01 and <0.05, respectively.

References

1. Borghi, N. *et al.* E-cadherin is under constitutive actomyosin-generated tension that is increased at cell-cell contacts upon externally applied stretch. *Proceedings of the National Academy of Sciences of the United States of America* **109**, 12568-12573 (2012).
2. Liu, Z. *et al.* Mechanical tugging force regulates the size of cell-cell junctions. *Proceedings of the National Academy of Sciences of the United States of America* **107**, 9944-9949 (2010).
3. Chen, C.S., Tan, J. & Tien, J. Mechanotransduction at cell-matrix and cell-cell contacts. *Annual review of biomedical engineering* **6**, 275-302 (2004).
4. Bernstein, B.W. & Bamburg, J.R. Actin-ATP hydrolysis is a major energy drain for neurons. *The Journal of neuroscience : the official journal of the Society for Neuroscience* **23**, 1-6 (2003).
5. Daniel, J.L., Molish, I.R., Robkin, L. & Holmsen, H. Nucleotide exchange between cytosolic ATP and F-actin-bound ADP may be a major energy-utilizing process in unstimulated platelets. *European journal of biochemistry / FEBS* **156**, 677-684 (1986).
6. Guilluy, C. *et al.* The Rho GEFs LARG and GEF-H1 regulate the mechanical response to force on integrins. *Nature cell biology* **13**, 722-727 (2011).
7. Marjoram, R.J., Guilluy, C. & Burridge, K. Using magnets and magnetic beads to dissect signaling pathways activated by mechanical tension applied to cells. *Methods* **94**, 19-26 (2016).
8. Barry, A.K. *et al.* alpha-catenin cytomechanics--role in cadherin-dependent adhesion and mechanotransduction. *J Cell Sci* **127**, 1779-1791 (2014).
9. Collins, C. *et al.* Localized tensional forces on PECAM-1 elicit a global mechanotransduction response via the integrin-RhoA pathway. *Current biology : CB* **22**, 2087-2094 (2012).
10. Kim, T.J. *et al.* Dynamic visualization of alpha-catenin reveals rapid, reversible conformation switching between tension states. *Current biology : CB* **25**, 218-224 (2015).
11. Bays, J.L. *et al.* Vinculin phosphorylation differentially regulates mechanotransduction at cell-cell and cell-matrix adhesions. *The Journal of cell biology* **205**, 251-263 (2014).
12. Tzima, E. *et al.* A mechanosensory complex that mediates the endothelial cell response to fluid shear stress. *Nature* **437**, 426-431 (2005).
13. Kishimoto, A., Ogura, T. & Esumi, H. A pull-down assay for 5' AMP-activated protein kinase activity using the GST-fused protein. *Molecular biotechnology* **32**, 17-21 (2006).
14. Zhou, G. *et al.* Role of AMP-activated protein kinase in mechanism of metformin action. *The Journal of clinical investigation* **108**, 1167-1174 (2001).
15. Walsh, S.V. *et al.* Rho kinase regulates tight junction function and is necessary for tight junction assembly in polarized intestinal epithelia. *Gastroenterology* **121**, 566-579 (2001).
16. Ivanov, A.I., Hunt, D., Utech, M., Nusrat, A. & Parkos, C.A. Differential roles for actin polymerization and a myosin II motor in assembly of the epithelial apical junctional complex. *Molecular biology of the cell* **16**, 2636-2650 (2005).
17. Sebbagh, M., Santoni, M.J., Hall, B., Borg, J.P. & Schwartz, M.A. Regulation of LKB1/STRAD localization and function by E-cadherin. *Current biology : CB* **19**, 37-42 (2009).
18. Yoshida, C. & Takeichi, M. Teratocarcinoma cell adhesion: identification of a cell-surface protein involved in calcium-dependent cell aggregation. *Cell* **28**, 217-224 (1982).
19. Nagafuchi, A., Shirayoshi, Y., Okazaki, K., Yasuda, K. & Takeichi, M. Transformation of cell adhesion properties by exogenously introduced E-cadherin cDNA. *Nature* **329**, 341-343 (1987).
20. Zheng, B. & Cantley, L.C. Regulation of epithelial tight junction assembly and disassembly by AMP-activated protein kinase. *Proceedings of the National Academy of Sciences of the United States of America* **104**, 819-822 (2007).

21. Zipfel, P.A., Zhang, W., Quiroz, M. & Pendergast, A.M. Requirement for Abl kinases in T cell receptor signaling. *Current biology : CB* **14**, 1222-1231 (2004).
22. le Duc, Q. *et al.* Vinculin potentiates E-cadherin mechanosensing and is recruited to actin-anchored sites within adherens junctions in a myosin II-dependent manner. *The Journal of cell biology* **189**, 1107-1115 (2010).
23. Chrzanowska-Wodnicka, M. & Burridge, K. Rho-stimulated contractility drives the formation of stress fibers and focal adhesions. *The Journal of cell biology* **133**, 1403-1415 (1996).
24. Amano, M. *et al.* Phosphorylation and activation of myosin by Rho-associated kinase (Rho-kinase). *The Journal of biological chemistry* **271**, 20246-20249 (1996).
25. Puszkin, S. & Rubin, E. Adenosine diphosphate effect on contractility of human muscle actomyosin: inhibition by ethanol and acetaldehyde. *Science* **188**, 1319-1320 (1975).
26. Shewan, A.M. *et al.* Myosin 2 is a key Rho kinase target necessary for the local concentration of E-cadherin at cell-cell contacts. *Molecular biology of the cell* **16**, 4531-4542 (2005).
27. Mehta, D. & Gunst, S.J. Actin polymerization stimulated by contractile activation regulates force development in canine tracheal smooth muscle. *The Journal of physiology* **519 Pt 3**, 829-840 (1999).
28. Cipolla, M.J., Gokina, N.I. & Osol, G. Pressure-induced actin polymerization in vascular smooth muscle as a mechanism underlying myogenic behavior. *FASEB J* **16**, 72-76 (2002).
29. Nash, R.W., McKay, B.S. & Burke, J.M. The response of cultured human retinal pigment epithelium to hypoxia: a comparison to other cell types. *Investigative ophthalmology & visual science* **35**, 2850-2856 (1994).
30. Kahn, B.B., Alquier, T., Carling, D. & Hardie, D.G. AMP-activated protein kinase: ancient energy gauge provides clues to modern understanding of metabolism. *Cell Metab* **1**, 15-25 (2005).
31. Balaban, R.S., Kantor, H.L., Katz, L.A. & Briggs, R.W. Relation between work and phosphate metabolite in the in vivo paced mammalian heart. *Science* **232**, 1121-1123 (1986).
32. Grashoff, C. *et al.* Measuring mechanical tension across vinculin reveals regulation of focal adhesion dynamics. *Nature* **466**, 263-266 (2010).
33. Kannan, N. & Tang, V.W. Synaptopodin couples epithelial contractility to alpha-actinin-4-dependent junction maturation. *The Journal of cell biology* **211**, 407-434 (2015).
34. Zhang, L., Li, J., Young, L.H. & Caplan, M.J. AMP-activated protein kinase regulates the assembly of epithelial tight junctions. *Proceedings of the National Academy of Sciences of the United States of America* **103**, 17272-17277 (2006).
35. Mammoto, T., Mammoto, A. & Ingber, D.E. Mechanobiology and developmental control. *Annual review of cell and developmental biology* **29**, 27-61 (2013).
36. Janmey, P.A., Wells, R.G., Assoian, R.K. & McCulloch, C.A. From tissue mechanics to transcription factors. *Differentiation; research in biological diversity* **86**, 112-120 (2013).
37. Klein, E.A. *et al.* Cell-cycle control by physiological matrix elasticity and in vivo tissue stiffening. *Current biology : CB* **19**, 1511-1518 (2009).
38. Levental, K.R. *et al.* Matrix crosslinking forces tumor progression by enhancing integrin signaling. *Cell* **139**, 891-906 (2009).
39. Gemayel, C. & Waters, D. Mechanical or metabolic treatment for coronary disease: synergistic, not antagonistic, approaches. *Cardiology in review* **10**, 182-187 (2002).
40. Rice, K.M. *et al.* Diabetes alters vascular mechanotransduction: pressure-induced regulation of mitogen activated protein kinases in the rat inferior vena cava. *Cardiovascular diabetology* **5**, 18 (2006).

Materials and Methods.

Cell lines. No cell lines used in this study were found in the database of commonly misidentified cell lines maintained by the ICLAD and NCBI. MCF10A human breast epithelial cells and MDCK II canine kidney epithelial cells were purchased from ATCC and were maintained as previously described[11,41]. Cell lines were used for no more than twelve passages and were tested periodically for mycoplasma contamination (Lonzo MycoAlert). The cell lines were not authenticated. MDCKII lines expressing control shLuc, shLKB1 clones 11 and 14, and shE-cadherin were generous gifts from Dr. Michael Sebbagh[17]. MDCKII cells were maintained in DMEM (4g/L D-glucose with L-Glutamine) with 10% FBS (Atlanta Biologicals) and 1x Penicillin/ Streptomycin (Sigma). These lines were chosen for they are both non-tumorigenic epithelial lines that form strong cell-cell adhesions which have been characterized by our laboratory and others[11,41-43]. 293GPG cells are a virus-producing cell line that are a derivative of 293T cells and were maintained as described previously[11].

Constructs. shRNA lentiviral particles targeting LKB1 and AMPK were purchased from Santa Cruz (270074-V labeled shLKB1, 29673-V denoted shAMPK1, and 45312-V termed shAMPK2). Additional control shRNA lentiviral particles containing scrambled AMPK targeting regions were purchased from Santa Cruz (108080, referred to as shControl). pLEGFP-vinculin Y822F was generated using site-specific mutagenesis of pLEGFP-WTvinculin[11,42].pGEX4T1-SAMS (aattccacatgaggtccgccatgtccggcttgcacctagtaaaac gacgac) and SAMA (aattccacatgaggtccgccatggccggcttgcacctagtaaaacgacgac) were generated by annealing oligonucleotides and ligating oligonucleotides into pGEX4T1 vector (GE Healthcare) cut at Xho1 and EcoR1 restriction sites. pGEX-RBD was a generous gift from Dr. Keith Burridge (University of North Carolina).

Magnetic Bead Force Assays. The application of tensile force to E-cadherin using magnetic beads was performed as previously described[11]. In brief, paramagnetic beads

were coated with Fc-Ecadherin, IgG or syndecan-1 antibodies. For the E-cadherin and IgG coated beads, 1.5 mg Dynabeads Protein A (Invitrogen) were coated with 10 µg purified Fc-E-cadherin[44] or IgG. For the syndecan experiments, 0.75 µg protein G Dynabeads (Invitrogen) were coated with 10µg syndecan-1 antibody (281.2; BD Biosciences). The beads were incubated with cells for 40 min at 37°C in the presence or absence of Compound C (10µM, Sigma), Blebbistatin (50µM, Sigma), or HECD-1 (200µg/mL, Invitrogen). Tensile forces were applied to beads 5-10 minutes using a permanent ceramic magnet. For all experiments, the magnet was placed parallel to and at a distance of 0.6 cm from the cell surface, so that the force on a single bead was approximately 10 pN[6,11]. After application of force, the cells were transferred to ice and immediately lysed.

Shear stress. To examine the cellular response to shear stress, cells were grown to 90-95% confluence on 35mm coverslips coated with 10µg/ml fibronectin. Cells were placed in a parallel plate flow chamber (Glycotech) and a Buchler polystatic pump was employed to apply force at 10dyn/cm^2 by administering media onto the cells at a rate of 3mL/minute. To determine force, the equation $\tau = 6\mu Q/a^2 b$ [45] was used. τ = shear stress, dynes/cm^2, μ= apparent viscosity of the media (DMEM-F12= 0.009598 Poise or dynes*sec/ cm^2), Q= volumetric flow rate (3 mL/min), a= channel height (0.12 cm), and b= channel width (2 cm). For signaling and cytoskeletal reinforcement studies, fluid was passed along the monolayer of cells for 6 hours in the presence or absence of Compound C (Sigma, 10µM), Oligomycin A (Tocris, 10µM), or Carbonyl cyanide-*4*-(trifluoromethoxy)phenylhydrazone (i.e. FCCP, Sigma, 1µM) or in low glucose media (0.5 g/L D-Glucose in DMEM). Cells were then immediately lysed in 2X Laemmli sample buffer or fixed in 4% paraformaldehyde. For glucose uptake assays, cells were exposed to shear stress for 2 hours and then allowed to recover for 1 hour with glucose derivative (2-NBDG).

Calyculin A Treatment. Cells were grown to near confluence and treated with 5nM of Calyculin A (Cell Signaling) for 40 minutes and then lysed.

Calcium-switch assays. The calcium-switch assays were performed by incubating cells in calcium-free media for 12 hours and then restoring calcium-containing media for the times indicated.

AMPK *in vitro* kinase assay. Cells with and without force applied were lysed into an *in vitro* kinase assay buffer (50 mM Tris, pH 7.4, 50 mM NaF, 5 mM Na pyrophosphate, 1 mM EDTA, 1 mM EGTA, 250 mM mannitol, 1% (v/v) Triton X-100, 1 mM DTT). AMPK was immunoprecipitated from whole cell lysates a 1:100 dilution of a polyclonal antibody against AMPK (2532), and the immunoprecipitates were washed with 50 mM Tris, pH 7.4, 150 mM NaCl, 50 mM NaF, 5 mM Na pyrophosphate, 1 mM EDTA, 1 mM EGTA. GST-SAMS and GST-SAMA fusion proteins were purified according to the manufacturer's instructions. After elution, proteins were concentrated using the Amicon Ultra 3,000 MWCO system (Millipore). 1 µg of purified SAMS and SAMA proteins were added to a kinase reaction mixture (1X Hepes- Brif buffer, 250 mM Na Hepes, pH 7.4, 5 mM DTT, 0.1%% Brij-35, 100 µM cold ATP, 300 µM AMP, 25 mM $MgCl_2$, and 10 μC_i ^{32}P-ATP). 20µL of the reaction mixture was next added to 5µL of washed protein A beads with bound AMPK. The reactions were incubated for 30 minutes at room temperature and stopped by adding 5X Laemmli sample buffer. The samples were boiled, analyzed by SDS-PAGE, and detected by autoradiography.

AMPK activator. Cells without force applied were treated with 100 µM of A-769662 (Selleck Chemical) which is a potent, reversible allosteric activator of AMPK. Cells were treated with the activator for 2 hours and then fixed and stained for immunofluorescence.

Immunoprecipitation. To immunoprecipitate E-cadherin or LKB1, cells were solubilized in Extraction Buffer (10 mM Tris-HCl, pH 7.6, 50 mM NaCl, 1% triton X-100, 5mM EDTA, 50 mM NaF, 20 µg/ml aprotinin, 2 mM Na_3VO_4, and 1 mM PMSF). Clarified cell lysates were incubated with 6 µg of E-cadherin (HECD-1, Invitrogen) or a 1:100 dilution of a polyclonal LKB1 (Cell Signaling 27D10) antibody, and the resulting antibody

complexes were recovered with Protein G or Protein A agarose (Sigma). To immunoprecipitate AMPK, cells were lysed in ice-cold RIPA buffer (50 mM Tris-HCl, pH 7.4, 1% NP-40, 0.5% Na-deoxycholate, 0.1% SDS, 150 mM NaCl, 2mM EDTA, 50mM NaF, 20 µg/ml aprotinin, 2 mM Na_3VO_4, and 1 mM PMSF). Clarified lysates were incubated with a 1:100 dilution of a polyclonal antibody against AMPK (Cell Signaling 2532). The complexes were recovered with Protein A agarose (Sigma).

Pulldown assays. Force was applied to cells using the magnetic bead approach described above with the exception that cells were pretreated for 2 hours with 50µM blebbistatin (Sigma) or 200µg/mL HECD-1 (Invitrogen). Cells were lysed in ice-cold lysis buffer (20 mM Tris at pH 7.6, 150 mM NaCl, 0.1% NP-40, 2 mM $MgCl_2$, 20 µg/ ml aprotinin). Cadherin-coated beads were isolated from the lysate using a magnet and washed three times with lysis buffer. The bound proteins were denatured and reduced in 2X Laemmli sample buffer and separated using SDS-PAGE.

RhoA assays. Active RhoA (RhoA-GTP) was isolated using a GST fusion protein with Rhotekin binding domain (GST-RBD) as detailed in Arthur and Burridge[46]. The GST-RBD domain binds specifically to GTP-bound, but not GDP-bound, RhoA proteins[47]. Cells were lysed in 50 mM Tris (pH 7.6), 500mM NaCl, 0.1% SDS, 0.5% DOC, 1% triton X-100, $MgCl_2$ and rotated for 30 minutes with 30 µg of purified GST–RBD bound to glutathione-Sepharose beads. The beads were washed in 50 mM Tris (pH 7.6), 150 mM NaCl, 1% Triton X-100, 10 mM $MgCl_2$ and the bound proteins were separated using SDS–PAGE.

Immunoblotting. Cell lysates were fractionated by SDS-PAGE and transferred to PVDF (Immobilon). The membranes were blocked in 5% milk (vinculin, E-cadherin), 5% BSA (AMPK, pAMPK, ACC, pACC) or 1% BSA (pVinculin, pCrkL, CrkL, MLC, pMLC, Abl) and subjected to Western blot analysis. AMPK was recognized using a polyclonal antibody from Cell Signaling (2532) that detects both the endogenous α-1 and α-2 isoforms of the catalytic subunit, but not the regulatory γ and β subunits. Phospho-AMPK was detected with an antibody that recognizes AMPK phosphorylated at Thr172 (Cell Signaling Technology, 40H9 2535 @ 1:1000 dilution). LKB1 was recognized with a

polyclonal antibody from Cell Signaling (27D10 @ 1:1000 dilution). ACC was recognized with a polyclonal antibody from Cell Signaling (C83B10 @ 1:1000 dilution); phospho-ACC was detected with an antibody that recognizes ACC phosphorylated at S79 (Cell Signaling Technology, D7D11@ 1:1000 dilution). Abl kinase was recognized using a polyclonal antibody raised against a peptide mapping the kinase domain from Santa Cruz (clone K-12, @ 1:250 dilution). E-Cadherin was immunoblotted with an HECD-1 mouse monoclonal antibody (Invitrogen 13-1700 @ 1:1000 dilution) or monoclonal antibody from (BD Transduction Labs @ 1:1000 dilution). Vinculin was detected with a monoclonal vinculin antibody (hVIN-1, Sigma @ 1:1000 dilution), and phosphorylated vinculin at Y822 was recognized with a rabbit polyclonal antibody (AB61071, Abcam @ 1:1000 dilution). CrkL was recognized with a polyclonal antibody raised against the C-terminus of human CrkL (C-20, Santa Cruz Biotechnology @ 1:250 dilution) and phospho-CrkL was immunoblotted with a polyclonal antibody that recognizes CrkL phosphorylated at Y207 (3181S, Cell Signaling Technology @ 1:1000 dilution). Phosphorylated myosin light chain (MLC) was detected with antibodies against phosphorylated serine 19 (3671, Cell Signaling @ 1:1000 dilution). MLC was also recognized with an antibody from Cell Signaling Technology (3672 @ 1:1000 dilution). The blots were visualized using chemoluminescence detection reagents (Pierce), and the signal was detected on x-ray film (Kodak) or a GE Image Quant LAS 400 Imager. Immunoblots were quantified using the ImageJ program, which measures the integrated density of bands corrected for background. Shown is the average ratio density from at least 3 experiments ± standard error of mean. A series of two-tailed student t-tests, heteroscedastic variance, normal distribution, were performed to determine statistical significance.

Immunofluorescence. Cells were fixed in 4% paraformaldehyde in phosphate buffered saline (PBS), permeabilized in 0.5% Triton X-100 in Universal buffer (UB) (150 mM NaCl, 50 mM Tris pH 7.6, 0.01% NaN_3) for 3 minutes, and washed in UB or PBS. Cells were blocked with 5% goat serum in UB for an hour at 37°C, incubated with a primary antibody for 1 hour at 37°C, washed with UB, and then incubated with secondary antibody for 1 hour at 37°C. F-actin was stained using phalloidin conjugated with Texas

Red at a 1:200 dilution (Life Technologies). E-cadherin was visualized by staining with HECD-1 (Invitrogen) at a 1:500 dilution, followed by FITC-conjugated goat anti-mouse IgG (H+L) (Jackson ImmunoResearch Laboratories, Inc) at a 1:500 dilution. To examine LKB1, cells were blocked in 1% BSA in UB and stained with LKB1 at 1:400 (Cell Signaling, 27D10). To examine vinculin, cells were blocked with 10% BSA in UB and stained with hVin-1(Sigma) and F79 (Millipore) at a 1:100 dilution and β-catenin (Sigma) at 1:750, was and incubated with Texas Red–conjugated donkey anti-rabbit IgG (H + L) at a 1:500 dilution (Jackson ImmunoResearch Laboratories, Inc.) and FITC–conjugated donkey anti-mouse IgG (H + L) at a 1:300 dilution (Jackson ImmunoResearch Laboratories, Inc.). Fluorescence images were captured at room temperature with a confocal microscope (model LSM 510; Carl Zeiss Micro Imaging, Inc.). We used a 63X objective (Carl Zeiss Micro Imaging, Inc.) with an NA of 1.2. Images were obtained using the LSM Image Browser (Carl Zeiss Micro Imaging, Inc.). To examine vinculin the Leica SP8 confocal microscope was used with a 40X objective. Quantifications of images were made using ImageJ. Fifty junctions were chosen at random measured at random over at least five fields of view. Data analyzer was blinded to image identity. A Dixon Q-test$_{95\%}$ was used to determine if data should be excluded. Graphs report the corrected fluorescence intensity of the regions of interest of interest. The corrected fluorescence intensity= integrated density- background (area of measurement times the mean intensity). Data represented as a box and whisker box with 90-10 percentile shown. Fold increase in intensity was calculated from the average corrected fluorescence intensity divided by the corrected fluorescence intensity from the untreated samples and is depicted as the average of 3 independent experiments.

Glucose uptake assays. Glucose uptake was measured using a kit from Cayman Chemical (600470). To determine uptake in response to tensile forces, $1.0x10^5$ cells/well were plated in 24-well plates and grown for two days. One hour prior to assay, cells were transferred to PBS with and without Compound C (10 μM, Sigma) or 200μg/mL HECD-1 (Invitrogen). 50 μg of Dynabeads Protein A (Invitrogen) coated in 0.4 μg Fc-E-cadherin or IgG were incubated with cells for 45 minutes at 37°C. Just prior to applying force on cells, 33 μg of glucose derivative (2-NBDG) was added to each

well. Force was applied to beads for 10 minutes, and then the cells were permitted to recover for 10 minutes at 37°C and lysed in 250µL of 10 mM Tris (pH 7.4), 50mM NaCl, 5mM EDTA, 50mM NaF, 1% triton X-100 and protease inhibitors. The lysate were centrifuged at 12,000 rpm for 5 minutes at 4 °C, and the resulting supernatant (200µL) was collected. An equal volume of Cell- Based Assay Buffer (Cayman Chemical, 10009322) was added to the collected supernatant. 100 µL of resulting solution were loaded into a 96-well plate in triplicate, and a fluorescence reading at 485/535 nm was taken (Biotek Synergy Neo model NEOALHPA B, Gen 5 software). To evaluate uptake in response to junction formation, $1.0x10^5$ cells/well were plated in 24-well plates and grown for 48 hours in calcium-containing media. After 48 hours, the cells were incubated in calcium-free media for 12 hours and calcium was restored for the times indicated. The cells were lysed and the amount of glucose uptake was measured as described above. The glucose uptake concentration was determined using a standard curve. Results are reported as µg/mL/$1x10^5$ cells.

ATP assays. Cells were plated at a density of 0.75 $x10^5$ for 2 days in 35mm dishes. An hour before applying force, cells were treated with Compound C (Sigma 10µM), Oligomycin A (Tocris, 10µM), 2-NBDG (fluorescently-labeled 2-deoxyglucose from Cayman Chemical, 150µg/mL). Dynabeads (0.15mg) coated with 1µg of Fc-E-cadherin or IgG were incubated with the cells for 45 minutes. Force was applied using a ceramic magnet for 10 minutes. Intracellular ATP levels were examined using a Fluorometric ATP assay kit from Abcam (ab83355). Cells were lysed in 200µL of ATP Assay Buffer, centrifuged at 12,000 rpm for 5 minutes at 4°C, and protein was removed from the supernatant using a 10 Kd spin column (Thermo Scientific). 5µL of the de-proteinated sample were added to ATP reaction mix in 96-well plates and a fluorescence reading at 535/587nm was made (Biotek Synergy Neo model NEOALHPA B, Gen 5 software).

Transepithelial electrical resistance. Cells were plated on Costar® 0.4 µm Polycarbonate membrane Transwell® 24-well plates and grown to confluence. The cells were then incubated in calcium free DMEM overnight. Growth media was added back to the cultures for the indicated times and transepithelial electrical resistance was measured in triplicate using a Millipore Voltmeter (MERS 000 01). Results are in $\Omega*cm^2$.

Statistics and Reproducibility. Statistical differences between groups of data were analyzed using a series of two-tailed unpaired Student *t*-tests. All experiments were completed at least three independent times. Key findings were repeated by at least two of the authors.

Data availability. All data supporting the findings of this study are available from the corresponding author on reasonable request.

References for Methods

41. Maiers, J.L., Peng, X., Fanning, A.S. & DeMali, K.A. ZO-1 recruitment to alpha-catenin--a novel mechanism for coupling the assembly of tight junctions to adherens junctions. *J Cell Sci* **126**, 3904-3915 (2013).
42. Peng, X., Cuff, L.E., Lawton, C.D. & DeMali, K.A. Vinculin regulates cell-surface E-cadherin expression by binding to beta-catenin. *J Cell Sci* **123**, 567-577 (2010).
43. Rodgers, L.S., Beam, M.T., Anderson, J.M. & Fanning, A.S. Epithelial barrier assembly requires coordinated activity of multiple domains of the tight junction protein ZO-1. *J Cell Sci* **126**, 1565-1575 (2013).
44. Chappuis-Flament, S., Wong, E., Hicks, L.D., Kay, C.M. & Gumbiner, B.M. Multiple cadherin extracellular repeats mediate homophilic binding and adhesion. *The Journal of cell biology* **154**, 231-243 (2001).
45. Bacabac, R.G. *et al.* Dynamic shear stress in parallel-plate flow chambers. *Journal of biomechanics* **38**, 159-167 (2005).
46. Arthur, W.T. & Burridge, K. RhoA inactivation by p190RhoGAP regulates cell spreading and migration by promoting membrane protrusion and polarity. *Molecular biology of the cell* **12**, 2711-2720 (2001).
47. Ren, X.D., Kiosses, W.B. & Schwartz, M.A. Regulation of the small GTP-binding protein Rho by cell adhesion and the cytoskeleton. *The EMBO journal* **18**, 578-585 (1999).

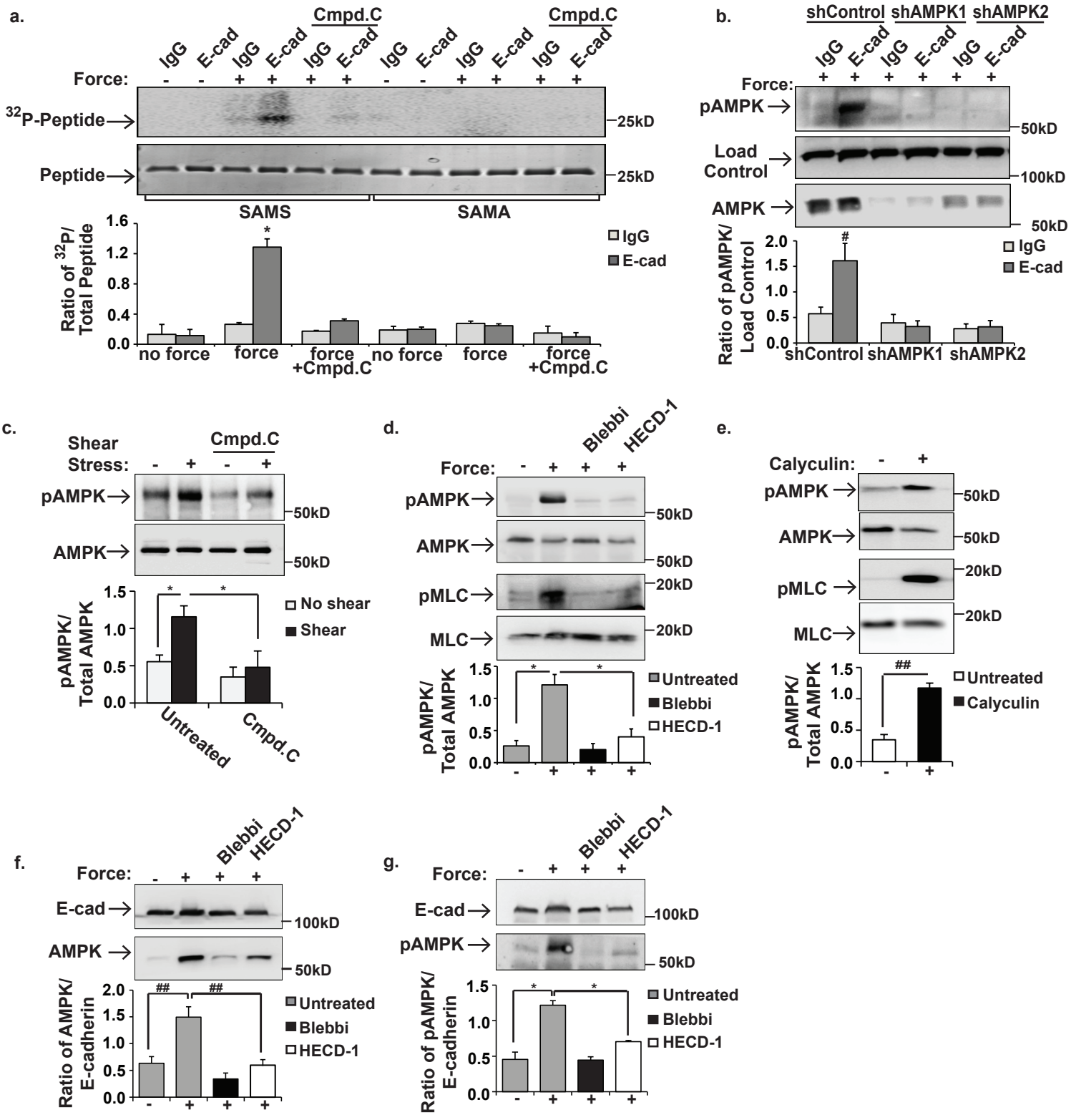
a.
Cmpd.C
Cmpd.C
IgG
E-cad
Force:
32P-Peptide
25kD
Peptide
25kD
SAMS
SAMA
Ratio of 32P/ Total Peptide
IgG
E-cad
no force
force
force +Cmpd.C
b.
shControl
shAMPK1
shAMPK2
Force:
pAMPK
50kD
Load Control
100kD
AMPK
50kD
Ratio of pAMPK/ Load Control
shControl
shAMPK1
shAMPK2
c.
Shear Stress:
Cmpd.C
pAMPK
50kD
AMPK
50kD
pAMPK/ Total AMPK
No shear
Shear
Untreated
Cmpd.C
d.
Blebbi
HECD-1
Force:
pAMPK
50kD
AMPK
50kD
pMLC
20kD
MLC
20kD
pAMPK/ Total AMPK
Untreated
Blebbi
HECD-1
e.
Calyculin:
pAMPK
50kD
AMPK
50kD
pMLC
20kD
MLC
20kD
pAMPK/ Total AMPK
Untreated
Calyculin
f.
Blebbi
HECD-1
Force:
E-cad
100kD
AMPK
50kD
Ratio of AMPK/ E-cadherin
Untreated
Blebbi
HECD-1
g.
Blebbi
HECD-1
Force:
E-cad
100kD
pAMPK
50kD
Ratio of pAMPK/ E-cadherin
Untreated
Blebbi
HECD-1

Figure 2. Bays et al 2017.

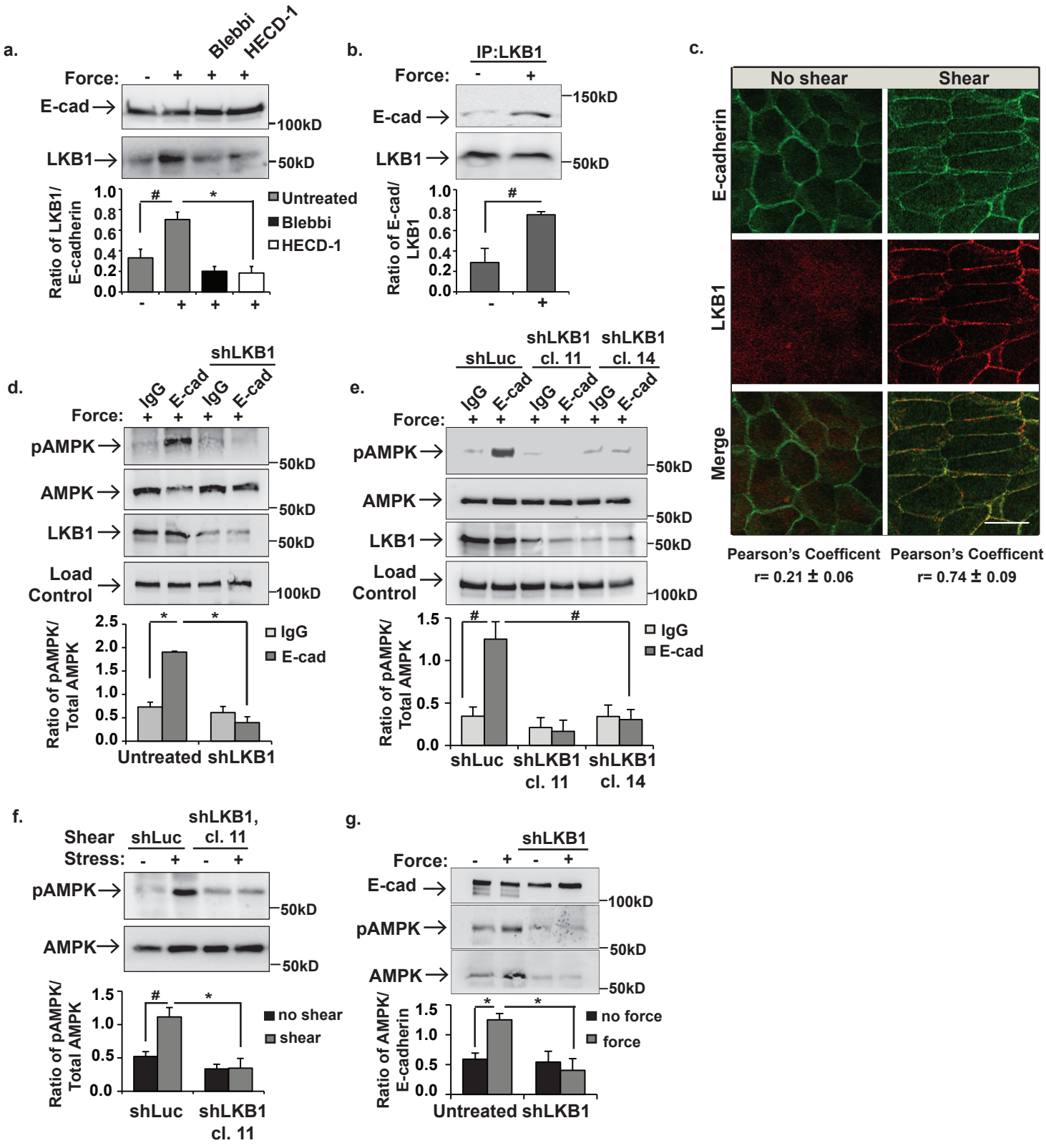

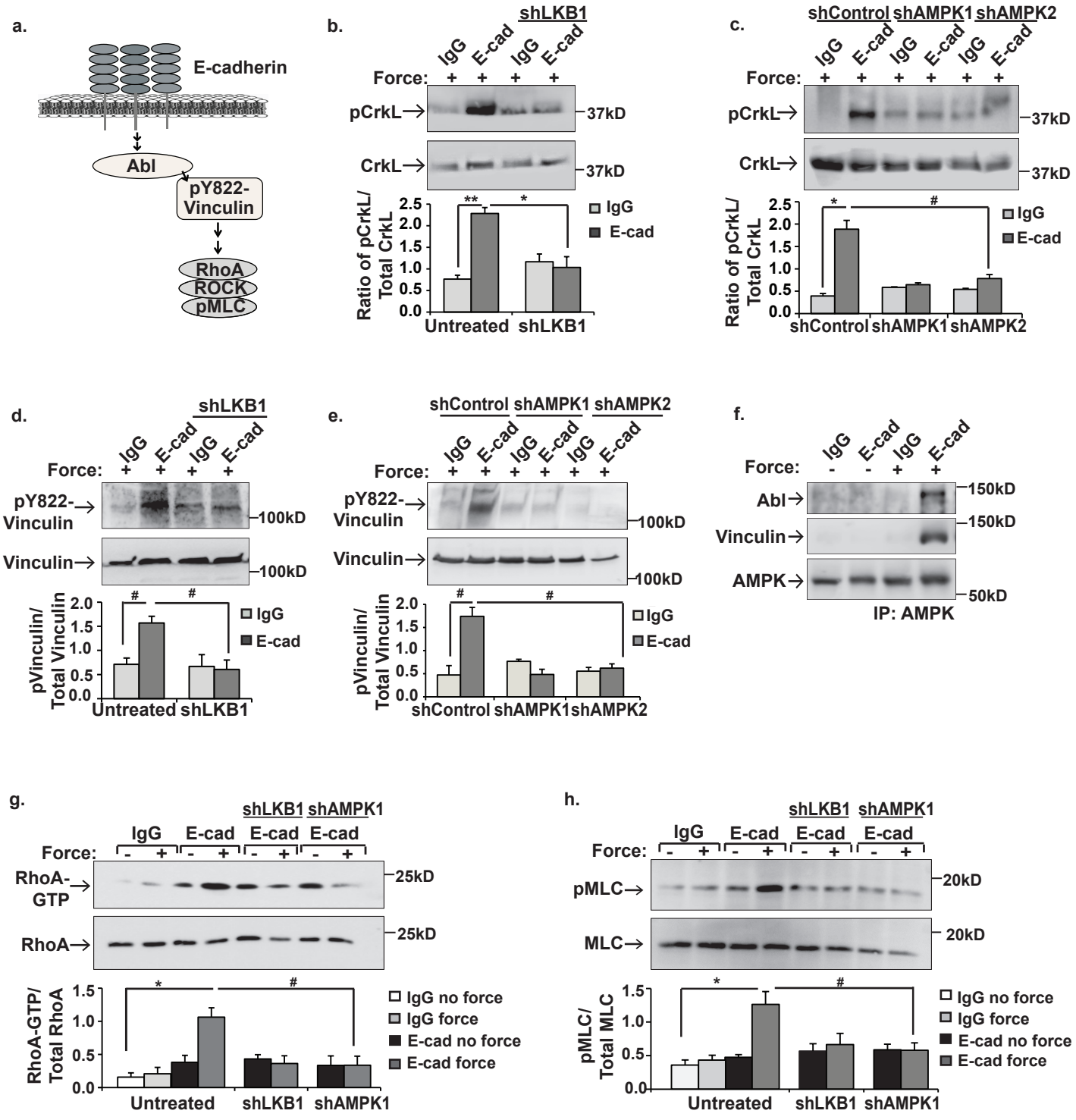
a.
E-cadherin
Abl
pY822-Vinculin
RhoA
ROCK
pMLC
b.
shLKB1
IgG
E-cad
Force:
pCrkL→
37kD
CrkL→
37kD
Ratio of pCrkL/ Total CrkL
IgG
E-cad
Untreated
shLKB1
c.
shControl
shAMPK1
shAMPK2
shControl
shAMPK1
shAMPK2
d.
pY822-Vinculin→
100kD
Vinculin→
100kD
pVinculin/ Total Vinculin
e.
f.
Abl→
150kD
Vinculin→
150kD
AMPK→
50kD
IP: AMPK
g.
RhoA-GTP→
25kD
RhoA→
25kD
RhoA-GTP/ Total RhoA
IgG no force
IgG force
E-cad no force
E-cad force
Untreated
shLKB1
shAMPK1
h.
pMLC→
20kD
MLC→
20kD
pMLC/ Total MLC

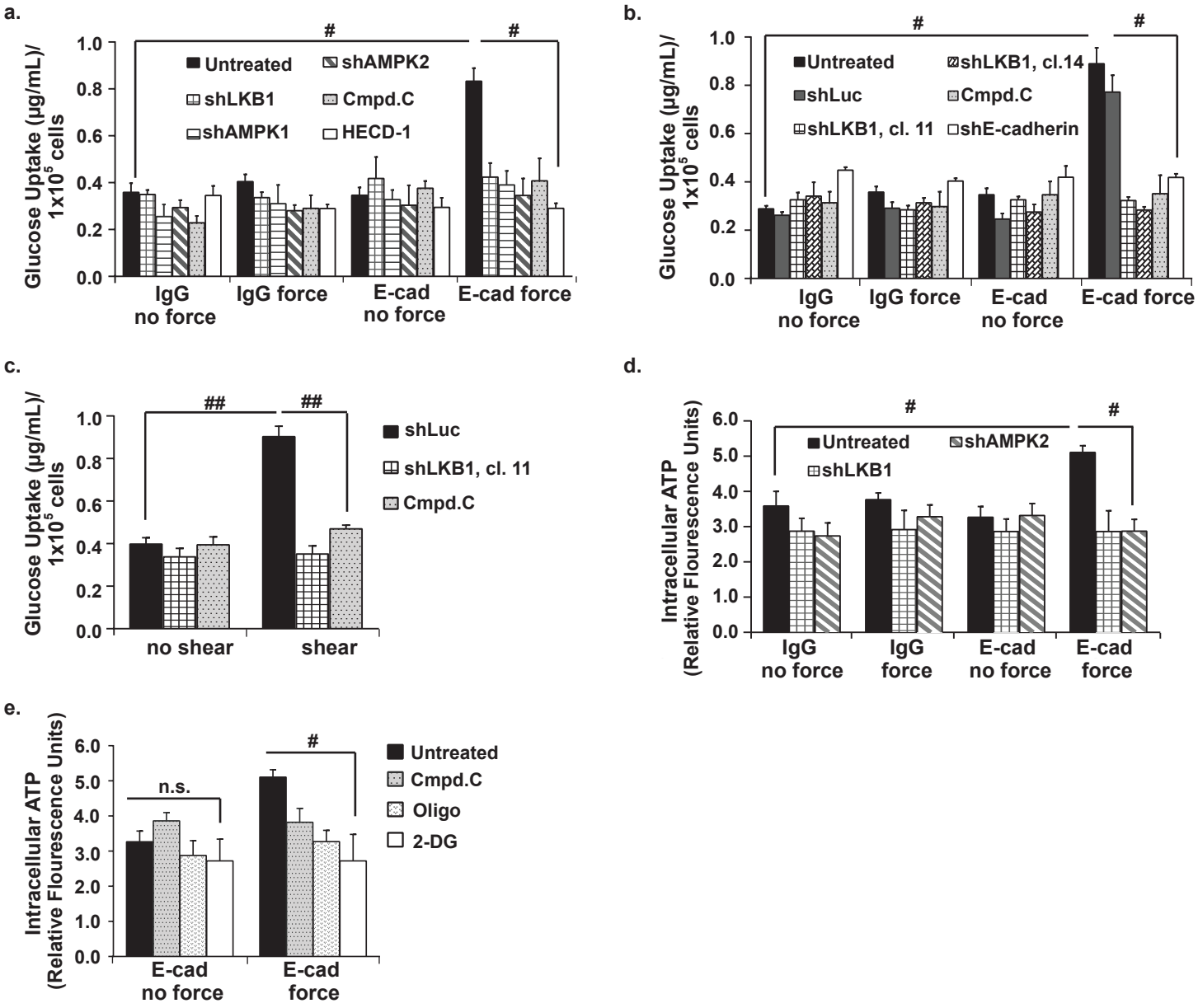
a.
Glucose Uptake (µg/mL)/ 1x10^5 cells
Untreated
shAMPK2
shLKB1
Cmpd.C
shAMPK1
HECD-1
IgG no force
IgG force
E-cad no force
E-cad force
b.
Glucose Uptake (µg/mL)/ 1x10^5 cells
Untreated
shLKB1, cl.14
shLuc
Cmpd.C
shLKB1, cl. 11
shE-cadherin
IgG no force
IgG force
E-cad no force
E-cad force
c.
Glucose Uptake (µg/mL)/ 1x10^5 cells
shLuc
shLKB1, cl. 11
Cmpd.C
no shear
shear
d.
Intracellular ATP (Relative Flourescence Units)
Untreated
shAMPK2
shLKB1
IgG no force
IgG force
E-cad no force
E-cad force
e.
Intracellular ATP (Relative Flourescence Units)
n.s.
Untreated
Cmpd.C
Oligo
2-DG
E-cad no force
E-cad force

Figure 5. Bays et al 2017

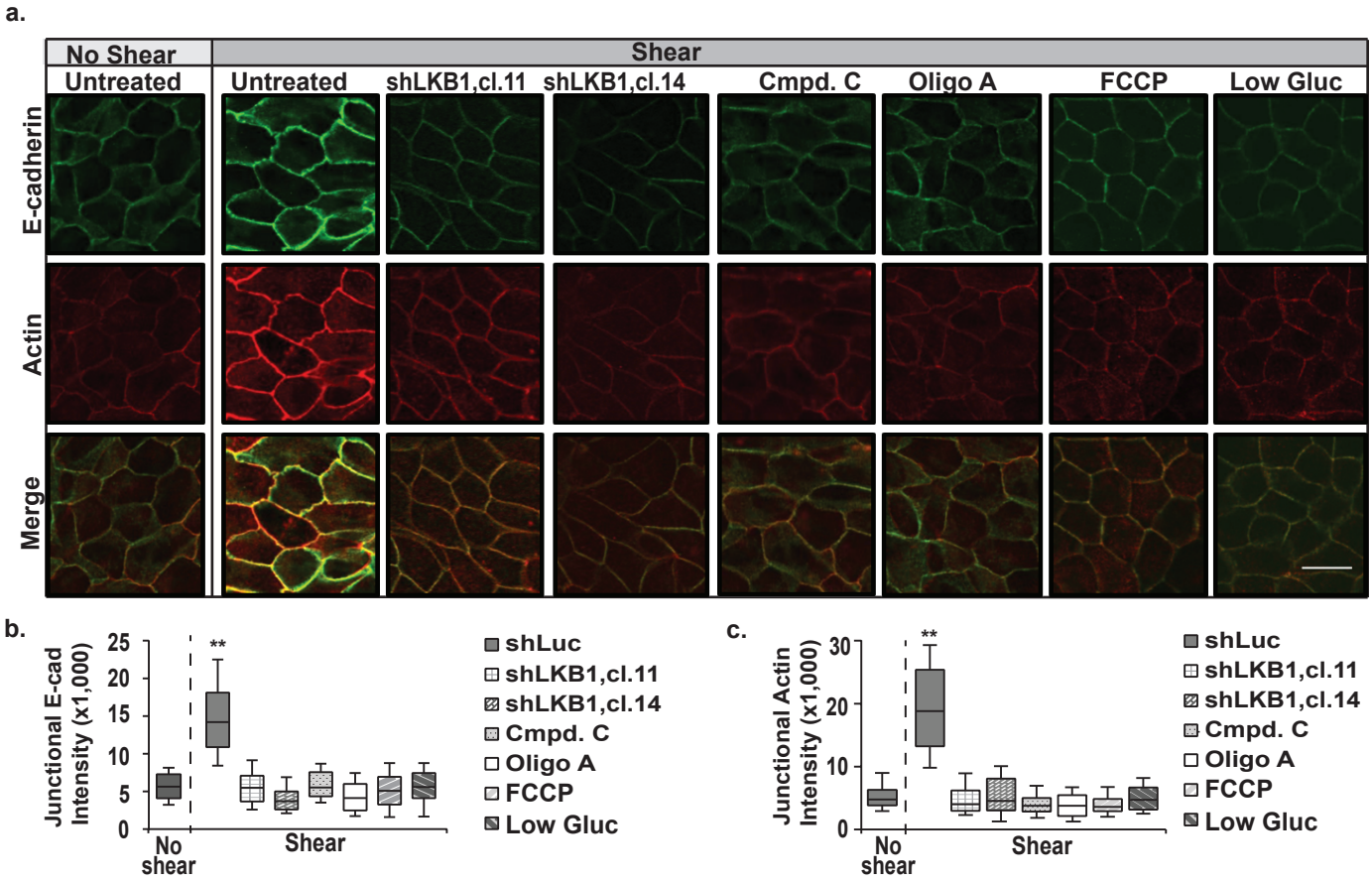

Legends to Supplementary Information

Supplementary Figure 1. The force-induced activation of AMPK occurs in multiple epithelial cell lines and requires E-cadherin and force transmission. MDCK II (**a,e**) or MCF10A (**b,c,f,g**) cells were incubated with magnetic beads coated with IgG (as a control), a syndecan-1 antibody, or E-cadherin extracellular domains (E-Cad). The cells were then left resting (-) or tensile forces were applied to the beads (+), the cells were lysed, and total cell lysates were immunoblotted with antibodies that recognize AMPK (a,b,d,e,f), pAMPK(a,b,d,e,f), acetyl CoA carboxylase (c,ACC), acetyl CoA carboxylase phosphorylated at its AMPK specific site (c, pACC), or E-cadherin (e, E-cad). shE-cad indicates cells with E-cadherin silenced. shAMPK indicates cells with E-cadherin silenced. Compound C (Cmpd. C), Blebbistatin (Blebbi) and HECD-1 indicate cells pretreated with these reagents. **d and h**, the assembly of cell-cell junctions was stimulated using a calcium switch assay, and the cells were lysed. The levels of pAMPK and AMPK were examined by immunoblotting (d) or E-cadherin was immunoprecipitated and AMPK association was monitored by immunoblotting (h). ' indicates minutes after Ca^{2+} re-addition. Steady indicates cells maintained in growth media. The graphs beneath the image show the average ± SEM for 3 independent experiments. **, *, and # indicate p values of <0.001, <0.01, and <0.05 , respectively. n.s. indicates not significant. Unprocessed scans of blots are shown in Supplementary Figure 5.

Supplementary Figure 2. LKB1 and AMPK are upstream of Abl-mediated phosphorylation of Y822 vinculin and RhoA contractility. MDCK II(**a**) or MCF10A(**b-e**) cells were incubated with magnetic beads coated with IgG (as a control) or E-cadherin extracellular domains (E-Cad). The cells were left resting (-) or tensile forces were applied to the beads (+), and the cells were lysed. **a and b**, immunoblots of whole cell lysates showing phosphorylation of CrkL at the Abl-specific site (pCrkL). shLKB1 denotes cells with LKB1 silenced. shLuc indicates cells expressing a control vector cDNA, and cl.11 and cl.14 indicate two different clonal cell lines lacking LKB1. **c**, immunoblots of whole cell lysates showing phosphorylation of vinculin Y822 (pY822). **d**, Active Rho (Rho–GTP) was isolated from whole cell lysates with GST–RBD and analyzed by western blotting. Compound C (Cmpd. C) indicates cells pretreated with this AMPK inhibitor. Y822F indicates MCF10A cells expressing a mutant vinculin containing a Y822F vinculin in place of the endogenous protein. **e**, immunoblots of whole cell lysates showing myosin light chain (MLC), or MLC phosphorylated in its regulatory chain (pMLC). The graphs beneath each image represent an average of three experiments ± SEM. **, *, # and ## indicate p values of <0.001, <0.01, < 0.05 and

<0.005, respectively. n.s. indicates not significant. Unprocessed scans of blots are shown in Supplementary Figure 5.

Supplementary Figure 3. Average fold activation of the glucose uptake and ATP values. Bar graphs displaying the average fold activation of force-induced glucose uptake assays (a-d) or of the intracellular ATP levels (e and f) are shown. **a-c**, The fold activations for the data presented in Figures 4a-c are shown in panels S3a, S3b, and S3c, respectively. **d**, the amount of glucose taken up into MCF10A cells after a calcium switch assay performed as described in supplemental Figure 1f. **e and f**, The fold activation for ATP levels presented in Figures 4d and e are shown in panels S3e and S3f, respectively. The values represent the average fold activation from three independent experiments ± the standard error of the mean.

Supplementary Figure 4. Controls for shear stress studies in Figure 5. a-h, MDCK II cells (n=79) or two clonal MDCK II cells lines (cl.11 and cl.14, n=51 and 76 respectively) lacking LKB1 were left untreated, treated with inhibitors of AMPK (Compound C=Cmpd. C, n=55), treated with inhibitors of ATP synthesis (Oligo A,n=53 or Carbonyl cyanide-4-(trifluoromethoxy)phenylhydrazone =FCCP,n=29), treated with inhibitors of myosin II (blebbistatin=Blebbi, n=30), treated with the AMPK activator (A-769662), or incubated in low glucose containing media (Low Gluc, n=25). The cells were left resting (no shear) or exposed to shear stress (shear). **a-d**, The cells were fixed, stained with antibodies against E-cadherin or with Texas-Red labelled phalloidin, and visualized using confocal microscopy. Representative images are shown in a and d. Scale bars=20 μm. The graph in b and c represent the average corrected fluorescence intensity of E-cadherin (b, E-cad) or F-actin (c) in junctions. The data are represented as a box and whisker plot with median, 10^{th}, 25^{th}, 75^{th}, and 90^{th} percentiles shown. **e,** the cells were fixed, stained with antibodies against vinculin or β-catenin, and examined by confocal microscopy. The graphs represent the average corrected fluorescence intensity of vinculin (**f**) or β-catenin (**g**) in junctions. **h,** the cells were lysed and total cell lysates were immunoblotted with antibodies against myosin light chain (MLC) or MLC phosphorylated at Serine 19 (pMLC). The graphs beneath each image represent an average of three experiments ± SEM. **, * and # indicate p values of <0.001, <0.01 and < 0.05, respectively. n.s. indicates not significant. Unprocessed scans of blots are shown in Supplementary Figure 5.

Supplementary Figure 5. Uncropped blots from Figures 1, 2, 3 and Supplementary figures 1**,** 2 and 4.

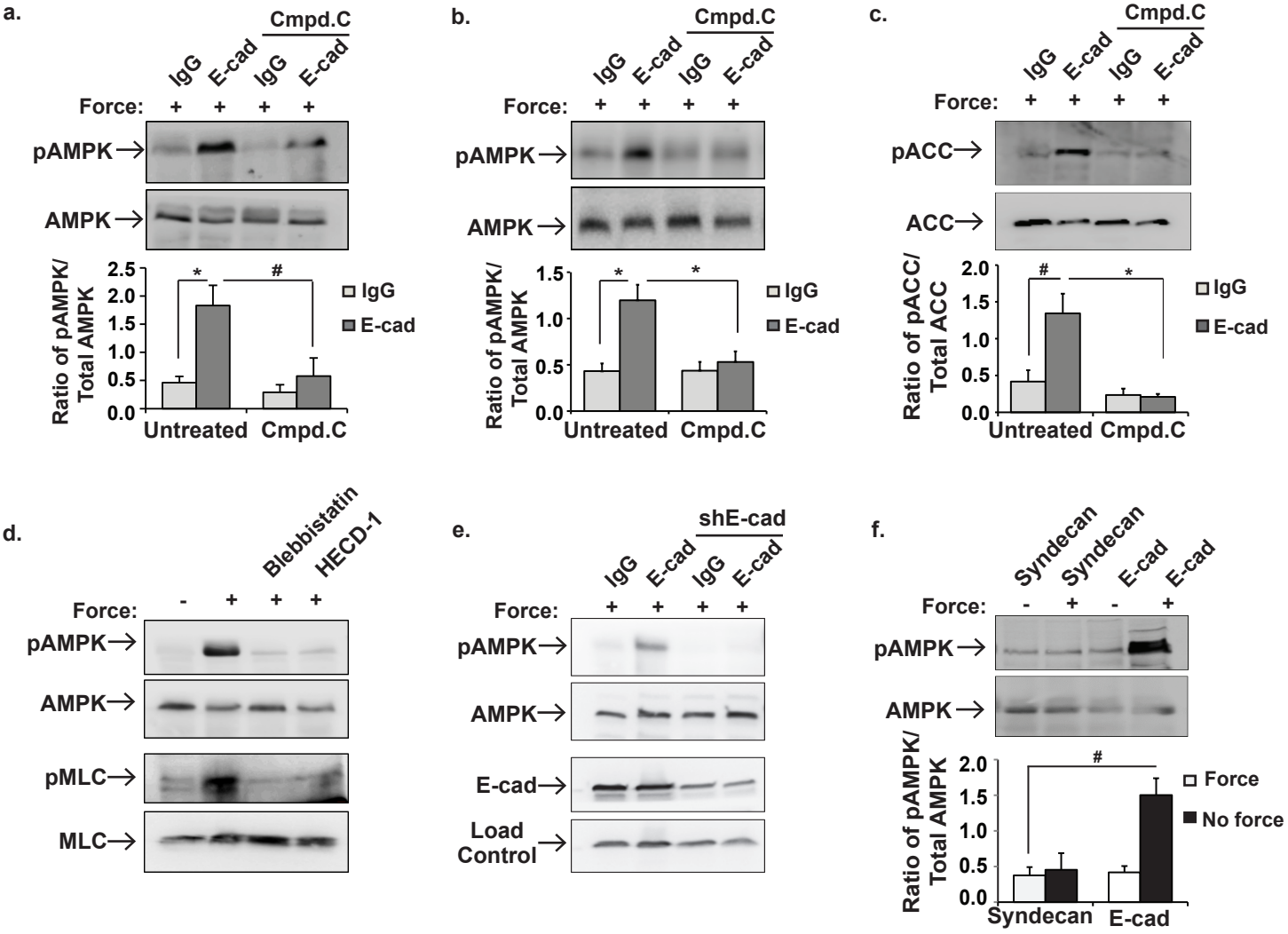
a.
Cmpd.C
IgG
E-cad
IgG
E-cad
Force: + + + +
pAMPK→
AMPK→
Ratio of pAMPK/ Total AMPK
2.5
2.0
1.5
1.0
0.5
0.0
*
#
IgG
E-cad
Untreated
Cmpd.C
b.
Cmpd.C
IgG
E-cad
IgG
E-cad
Force: + + + +
pAMPK→
AMPK→
Ratio of pAMPK/ Total AMPK
1.5
1.0
0.5
0.0
*
*
IgG
E-cad
Untreated
Cmpd.C
c.
Cmpd.C
IgG
E-cad
IgG
E-cad
Force: + + + +
pACC→
ACC→
Ratio of pACC/ Total ACC
2.0
1.5
1.0
0.5
0.0
#
*
IgG
E-cad
Untreated
Cmpd.C
d.
Blebbistatin
HECD-1
Force: - + + +
pAMPK→
AMPK→
pMLC→
MLC→
e.
shE-cad
IgG
E-cad
IgG
E-cad
Force: + + + +
pAMPK→
AMPK→
E-cad→
Load Control→
f.
Syndecan
Syndecan
E-cad
E-cad
Force: - + - +
pAMPK→
AMPK→
Ratio of pAMPK/ Total AMPK
2.0
1.5
1.0
0.5
0.0
#
Force
No force
Syndecan
E-cad

Supplemental Figure 2. Bays et al 2017

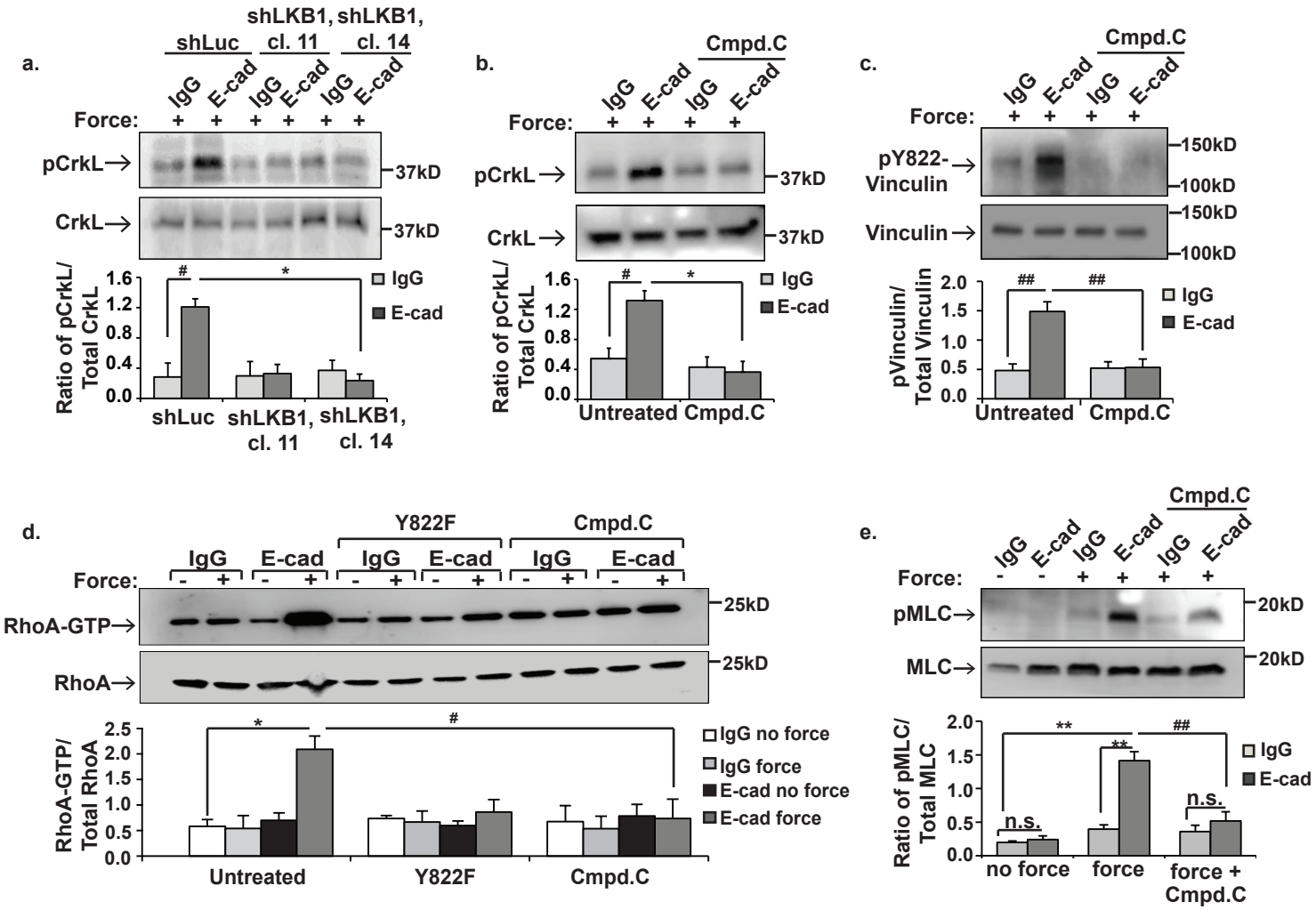

Supplemental Figure 3. Bays et al 2017

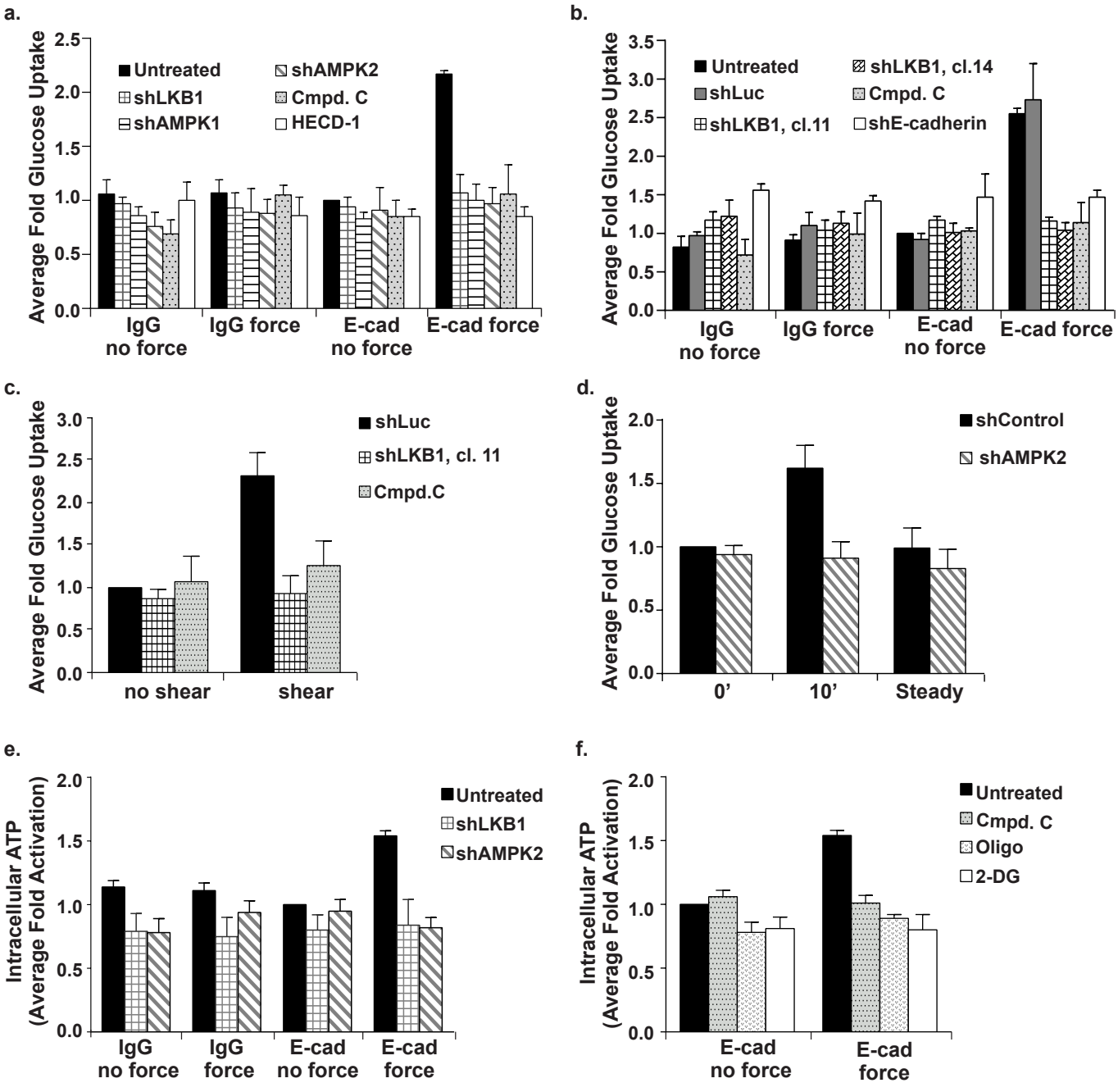

Supplemental Figure 4. Bays et al 2017.

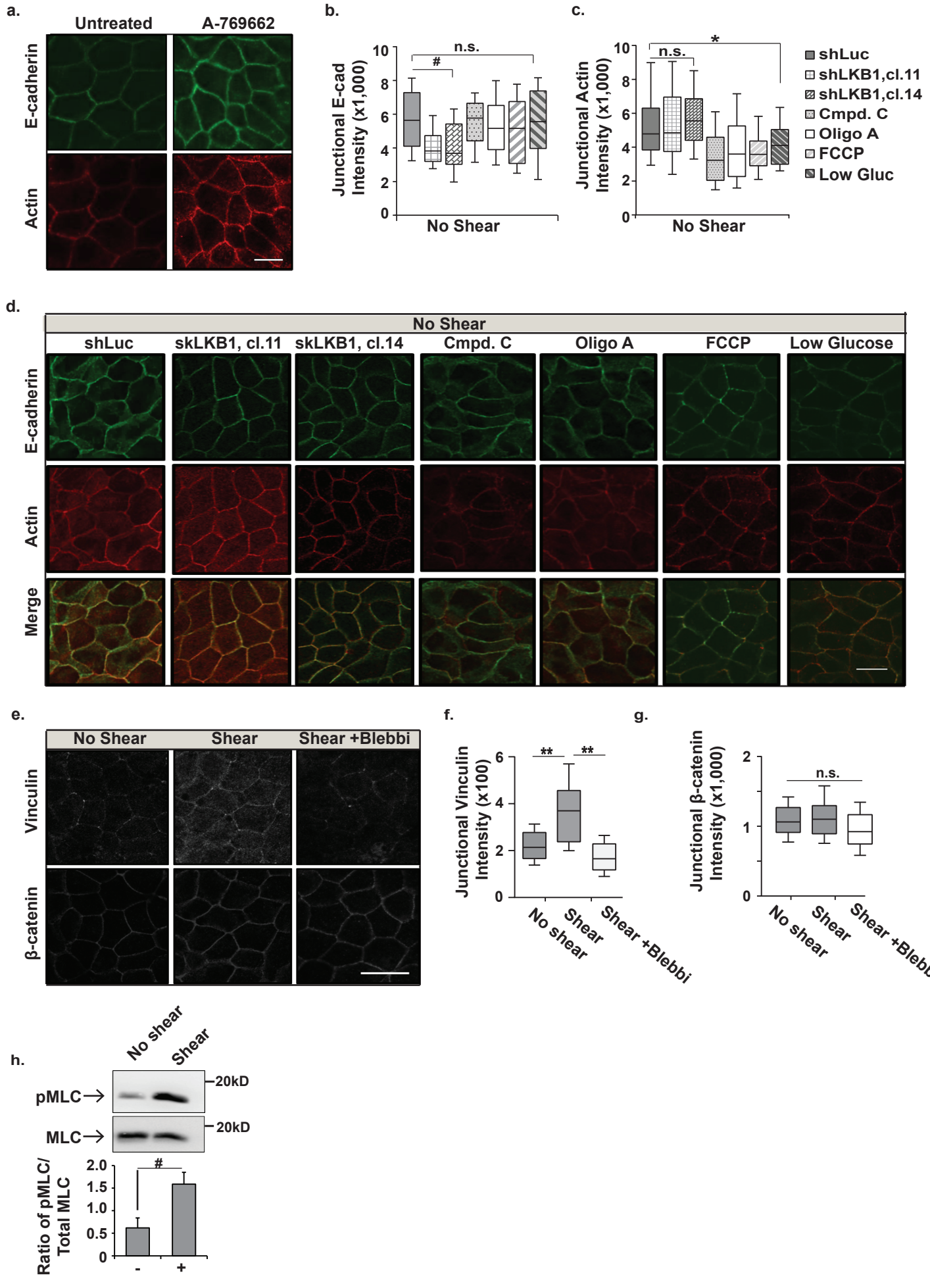

Supplemental Figure 5. Bays et al 2017.

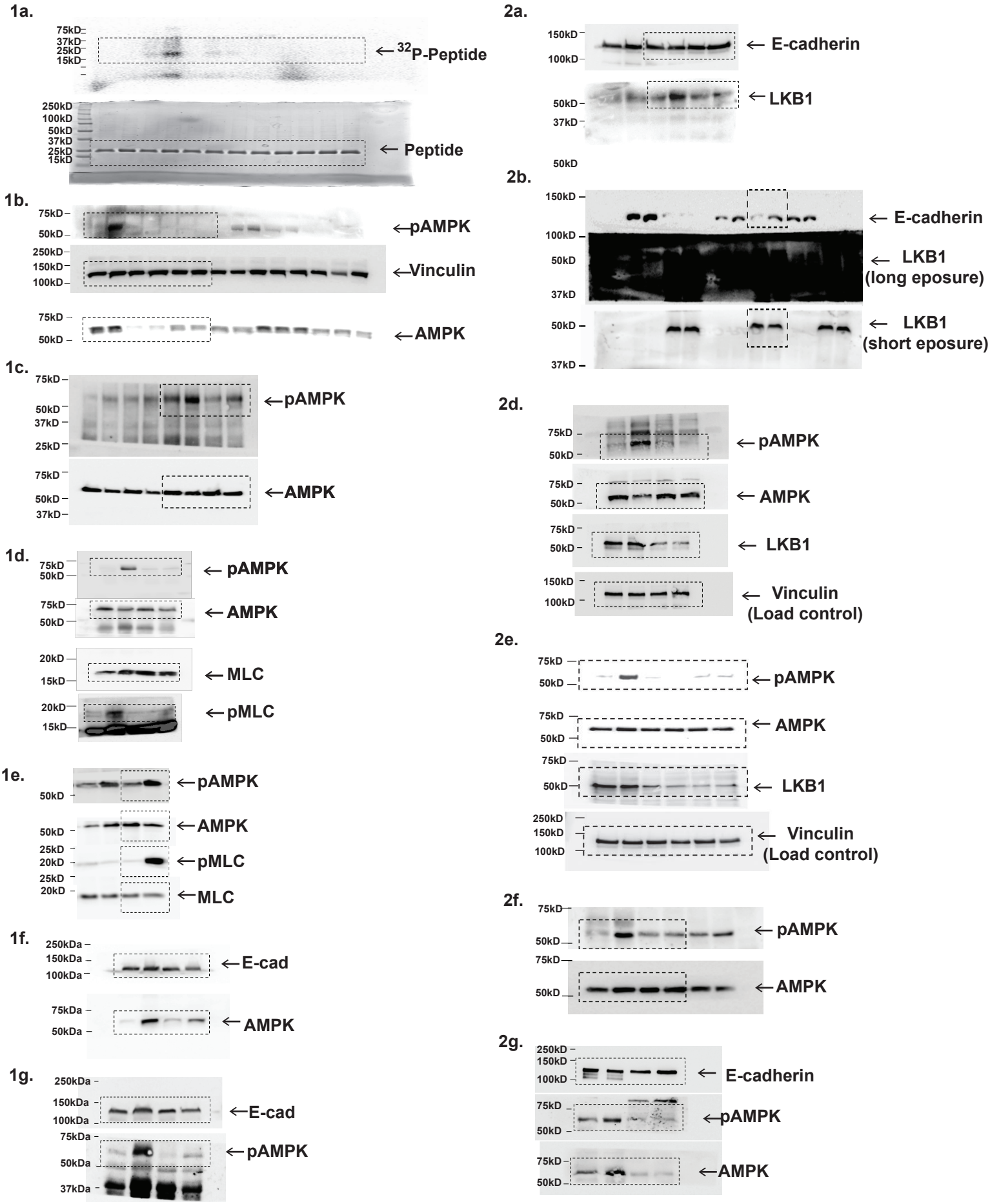

3b.

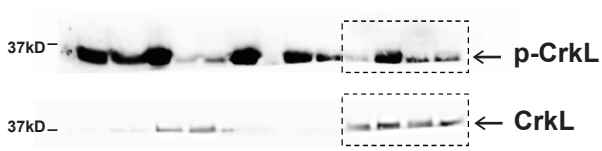

3c.

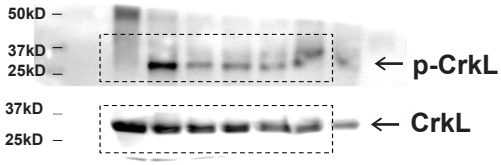

3d.

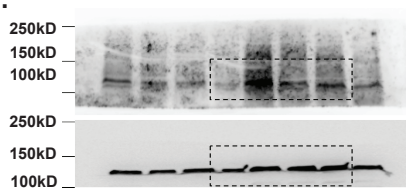

3e.

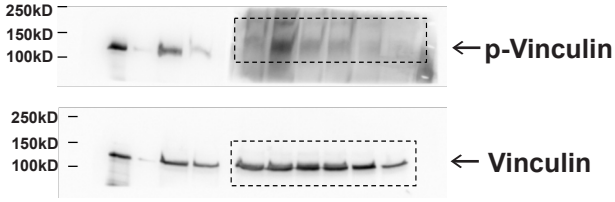

3f.

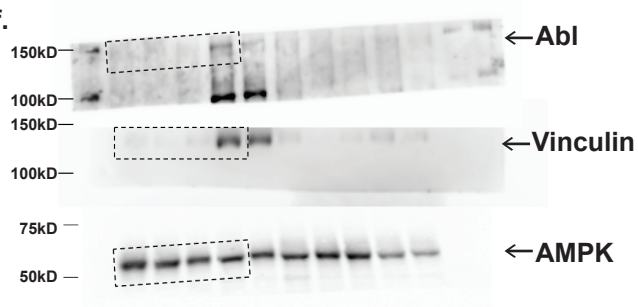

3g.

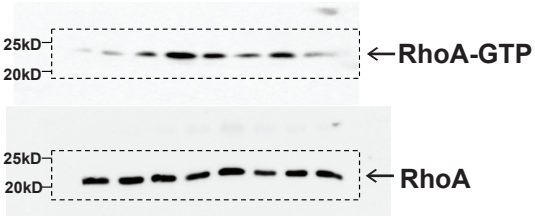

3h.

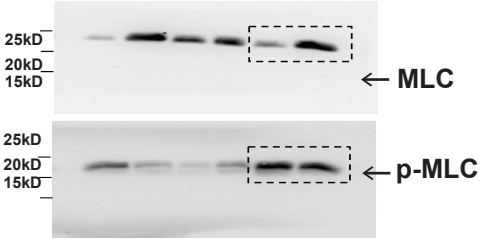

S1a.

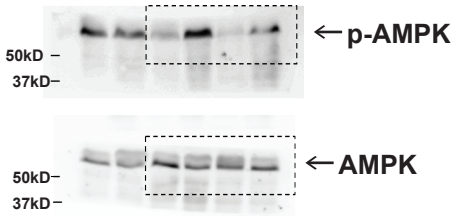

S1b.

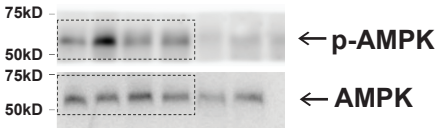

S1c.

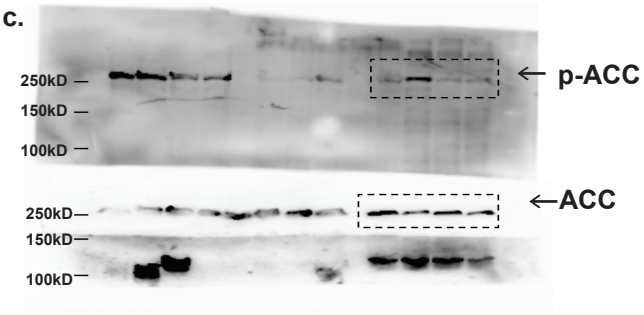

S1d.

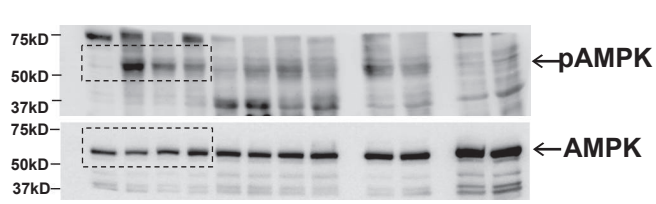

S1e.

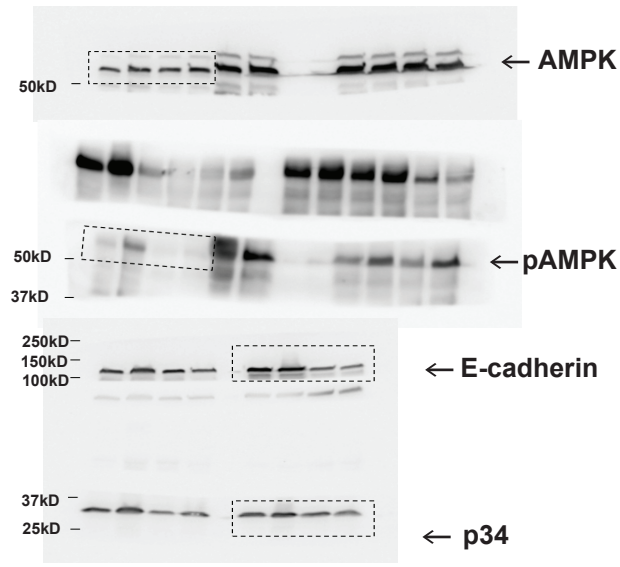

S1f.

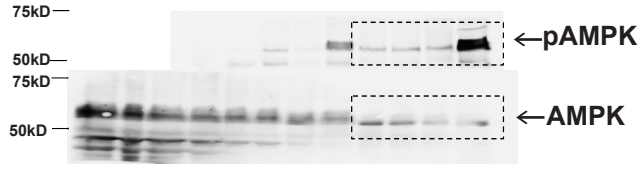

S1g.

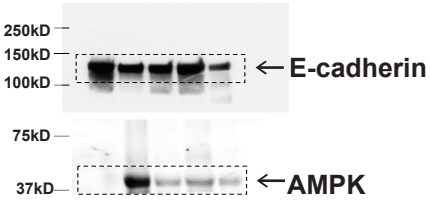

S1h.

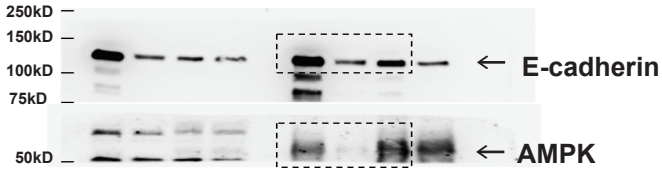

S2a.

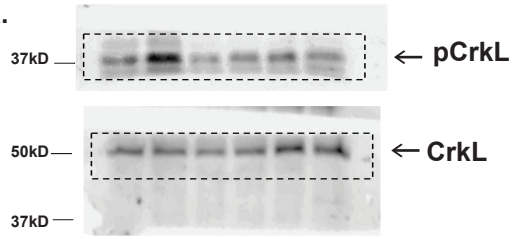

S2b.

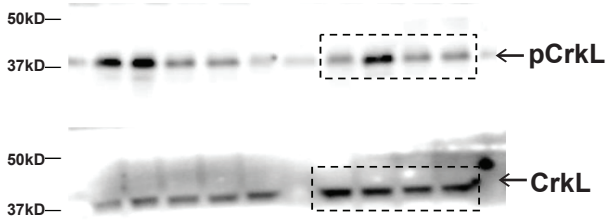

S2c.

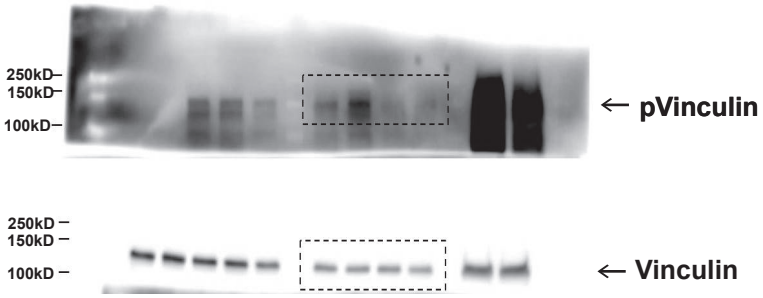

S2d.

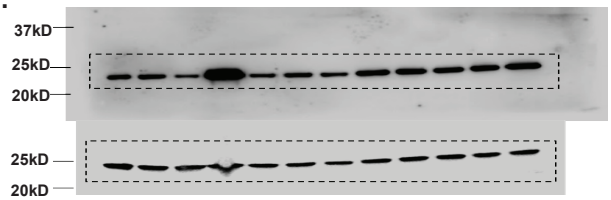

S2e.

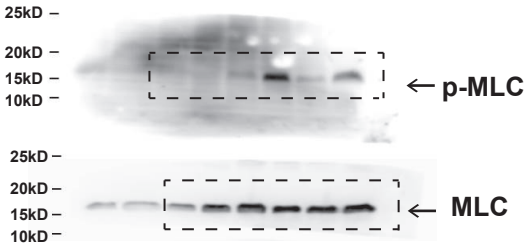

S4h.